2015-01-01

A Methodology For Use Of Digital Image Correlation For Hot Mix Asphalt Testing

Estefany Ramos
University of Texas at El Paso, eramos8@miners.utep.edu

A METHODOLOGY FOR USE OF DIGITAL IMAGE CORRELATION FOR HOT MIX ASPHALT TESTING

ESTEFANY RAMOS

Department of Civil Engineering

APPROVED:

Soheil Nazarian, Ph.D., Chair

Imad Abdallah, Ph.D.

Calvin Stewart, Ph.D.

Charles Ambler, Ph.D.
Dean of the Graduate School

Dedication

I would like to dedicate this thesis to my parents.

A METHODOLOGY FOR USE OF DIGITAL IMAGE CORRELATION FOR HOT MIX ASPHALT TESTING

by

Estefany Ramos, EIT, BSCE

THESIS

Presented to the Faculty of the Graduate School of

The University of Texas at El Paso

in Partial Fulfillment

of the Requirements

for the Degree of

MASTER OF SCIENCE

Department of Civil Engineering

THE UNIVERSITY OF TEXAS AT EL PASO

December 2015

Acknowledgements

I would first and foremost like to thank my thesis advisor, Dr. Soheil Nazarian, for his guidance and constant support throughout my graduate career. Without his advice and faith in me this thesis would have not been possible. It has been an honor to work under his supervision. I would also like to thank Dr. Imad Abdallah for helping me to not give up even when things didn't go as planned. Having his support was instrumental for this thesis. I am especially grateful for all the help I received from all of the staff at CTIS, especially Dr. Cesar Tirado and Sergio Rocha. I would also like to thank all of my fellow CTIS colleagues, specifically Victor Garcia and Pablo Cobos, for their constant help and for helping me make this thesis possible.

I would also like to extend my gratitude to Dr. Calvin Stewart for his advice and for allowing me to use his equipment. I would also like to thank his research assistants for their help and support.

Finally I would like to thank my family, especially my father, Telesforo Ramos, and my mother Yolanda Ramos, for always supporting and encouraging me. I would never have been able to go this far without them. Lastly, I want to thank my best friend for always being there for me, especially when I needed it the most.

"This material is based upon work supported by the National Science Foundation under Grant No. #10-60-113"
"Any opinions, findings, and conclusion or recommendations expressed in this material are those of the author(s) and do not necessarily reflect the views of the National Science Foundation."

Abstract

Digital Image Correlation (DIC) is a relatively new technology which aids in the measurement of material properties without the need for installation of sensors. DIC is a noncontact measuring technique that requires the specimen to be marked with a random speckled pattern and to be photographed during the test. The photographs are then post-processed based on the location of the pattern throughout the test. DIC can aid in calculating properties that would otherwise be too difficult even with other measuring instruments.

The objective of this thesis is to discuss the methodology and validate the use of DIC in different hot mix asphalt (HMA) tests, such as, the Overlay Tester (OT) Test, Indirect Tensile (IDT) Test, and the Semicircular Bending (SCB) Test. The DIC system provides displacements and strains in any visible surface. The properly calibrated 2-D or 3-D DIC data can be used to understand the complex stress and strain distributions and the modes of the initiation and propagation of cracks. The use of this observational method will lead to further understanding of the complex boundary conditions of the different test, and therefore, allowing it to be implemented in the analysis of other materials. The use of digital image correlation will bring insight and knowledge onto what is happening during a test.

Table of Contents

List of Tables

List of Figures

Chapter 1: Introduction

Digital Image Correlation is a relatively new technology that is being used as a noncontact technique to measure the mechanical responses of materials. The conventional measuring devices such as the linear variable differential transformers (LVDT) are proving to not be sufficiently adequate to capture all the information that is being developed during a test. DIC facilitates the process of obtaining the variation of the displacement and strain fields remotely in the HMA specimens without the need for installing contact sensors. DIC works by tracking a pattern that is painted on the specimen in photographs that are taken during a test. Given the complex stress and strain fields associated with different HMA tests and given the capabilities shown by DIC the objective of this thesis is to demonstrate the effective use of DIC in the different HMA tests as a reliable measuring technique. The focus of this thesis is to identify what procedures and analyses give the best results in the use of DIC of HMA mixes in three different tests, OT, IDT and SCB.

1.1 Literature Review

The difficulty of measuring material parameters adequately during laboratory tests has been the subject of several studies. Problems, such as the difficulty of attaching measuring instruments (such as LVDTs) to laboratory specimens can lead to some uncertainty in the measurements. Daniel et al. (2002) conducted a study on issues affecting the measurement of hot mix asphalt modulus. The main concern of the authors was the significant change in measurements due to noise and drift of the LVDTs during the test. Results showed that the dynamic moduli differed by up to a factor of 4.5 between the measurements from the actuator LVDT and the on-specimen LVDT. Chehab et al. (2007) pointed out the limitations of LVDTs such as the capability of only acquiring a limited amount of information at one point on a specimen. In that study DIC

was used to measure the fracture process zone strains to try to extend the validity of the viscoelastoplastic continuum damage (VEPCD) model. The VEPCD model was calibrated using measurements from LVDTs, but since the LVDTs could not capture the localized process zone strains, the VEPCD model ceased to accurately predict the performance of the asphalt mixtures after strain localization. The authors successfully used the DIC and LVDT measurements to calibrate the VEPCD model. The results showed that DIC-LVDT based model could accurately predict strains even beyond the localization up to the instance of macro-crack development and propagation. Thanks to the rapid development of the technology in the past few decades, engineers and scientists have developed software applications for the use of digital image correlation (DIC) to address these types of issues.

DIC has been successfully used in different materials to measure their properties, such as displacements, strains, and Poisson's ratio (Zhou et al., 2003, Hild et al., 2006, Chehab et al., 2007, and Tan et al., 2012*)*. Laurin et al. (2012) used DIC to understand the failure and damage mechanisms of composite materials such as carbon fibers and polymer matrix, which are used in aircrafts. The DIC method allowed them to validate boundary conditions, crosscheck measurements obtained with other techniques, improve the understanding of failure mechanisms, and to validate predictions of finite element simulations. Choi et al. (1997) used DIC to study concrete fracture during compressive loads. In that study, DIC was successfully applied to measure nonuniform deformations on the surface of concrete specimens in compression. Youngguk et al. (2002) successfully applied the DIC technique to the mechanical testing of HMA. The authors were able to compare and verify the DIC results with LVDT measurements. The authors also found that the DIC could be applied to cylindrical specimens.

The overlay tester (OT) was developed in the 1970s to evaluate the reflective cracking resistance of asphalt overlays (Germann et al., 1979). The OT measures the number of cycles to failure of the HMA specimens by simulating the opening and closing of joints and/or existing cracks induced by the vehicle loading (Zhou et al., 2003). Several research studies have deemed the OT test as reliable (Bennert et al., 2008, Bennert et al., 2009, Hajj et al., 2010). However, the reported repeatability of the results of the OT is considered as one of the main challenges in reliably evaluating the cracking resistance of the asphalt mixtures. Walubita et al. (2010) found that most of the variability in the results occurred because of inconsistencies in the laboratory testing as well as the sample preparation and machine calibration. Walubita et al. (2012) noted that tensile cracking tests in general have variability in their results due to assuming the fracture zone in the middle of the specimen. Garcia and Miramontes (2015) experimentally studied several potential sources of variability such as the specimen preparation (amount of glue, glue curing time, curing time of the specimen, and the gap spacing between the two base plates) and testing mechanism (specimen experiencing bending).

The indirect tensile (IDT) test is performed by loading a specimen across its vertical diametral plane at a rate of 50 mm/min (ASTM D6931). The strength of a specimen by the IDT is computed from the peak load at failure. Yi-qui et al. (2012) used DIC on HMA specimens subjected to IDT test to investigate their deformation and fracture properties. They found that digital image correlation could be used to obtain the strain fields of different asphalt mixtures, which made it possible to investigate the deformation and fracture properties accurately. Kim et al. (2002) used DIC to determine the proper gauge length for a 100-mm diameter IDT specimen. They concluded that a 50 mm gauge length was the best option for a 100-mm diameter IDT

specimen. The authors were also able to demonstrate that DIC is a good alternate to LVDT for deformation and strain measurements.

Chong and Kuruppu (1984) proposed the SCB test first for the fracture toughness determination of rocks and other materials. Gao et al. (2014) successfully used DIC with SCB specimens of Laurentian granite. Crack propagation velocity, fracture initiation toughness and fracture propagation toughness were calculated from the data obtained from DIC. The authors found that the DIC results were consistent with the results from the strain gauge measurements. Aragao et al. (2011) characterized fracture properties of HMA based on cohesive zone modeling and DIC. They simulated the DIC results during the SCB fracture tests using finite element analysis incorporated with material viscoelasticity and cohesive zone fracture. The authors concluded that DIC accurately captured the crack tip fracture process and could be incorporated to the numerical cohesive zone fracture modeling to identify fracture characteristics of HMAs.

1.2 Study and Materials

This study consisted of performing three different HMA testing with three difference types of mixes using DIC. Table 1.1 shows the three different mixes. Table 1.2 shows the gradation for each mix. These mixes include, Type D, Superpave D (SPD), and Thin Overlay Mixture (TOM). All mixes conform to Texas Department of Transportation (TxDOT) standards. The main purpose of performing three test is to prove the consistency between tests and therefore validate of the use of DIC for HMA testing. Table 1.3 describes each specimen by material, test, and air voids.

Table 1.1 Information of Different HMA Mixes

Mix Type	Location	Asphalt Binder	Asphalt Content, %	Asphalt Binder Source
Superpave Fine Mixture (SP D)	Abilene	PG-64-22	5.3	Alon
Traditional Fine Mixture (Type D)	Brownwood	PG-64-22	5.1	Jebro
Thin Overlay Mix (TOM)	Austin	PG-76-22	6.5	NA

Table 1.2 Gradation Chart for Different Mixes

Sieve Size	SPD	TOM	Type D
3/4"	100	100	100
1/2"	99.83	100	100
3/8"	97.71	98.9	98.5
No. 4	62.92	47.3	68
No. 8	35.94	21.8	37.5
No. 16	19.03	16.5	-
No. 30	15.42	12.9	15.5
No. 50	8.75	10.6	11
No. 200	3.28	6.3	3.4

Table 1.3 Specimen ID and Material

Material	ID	Air Voids (%)	Material	ID	Air Voids (%)
OT Cyclic TOM	Specimen 1	6.6	SCB TOM	Specimen 19	6.7
	Specimen 2	6.1		Specimen 20	6.8
	Specimen 3	6.1		Specimen 21	6.6
OT Cyclic SPD	Specimen 4	7.6	SCB SPD	Specimen 22	7.2
	Specimen 5	7.4		Specimen 23	7.2
	Specimen 6	7.8		Specimen 24	7.7
OT Cyclic Type D	Specimen 7	6.7	SCB Type D	Specimen 25	6.3
	Specimen 8	6.5		Specimen 26	6.6
	Specimen 9	6.5		Specimen 27	6.5
OT Monotonic TOM	Specimen 10	6.1	IDT TOM	Specimen 28	6.5
	Specimen 11	6.3		Specimen 29	6.0
	Specimen 12	6.3		Specimen 30	6.7
OT Cyclic SPD	Specimen 13	7.9	IDT SPD	Specimen 31	7.3
	Specimen 14	8.0		Specimen 32	7.0
	Specimen 15	7.8		Specimen 33	7.1
OT Monotonic Type D	Specimen 16	7.9	IDT Type D	Specimen 34	7.2
	Specimen 17	6.9		Specimen 35	6.8
	Specimen 18	6.8		Specimen 36	6.9

Chapter 2: DIC Methodology

The purpose of this chapter is to describe in detail the methodology followed to implement successfully DIC on HMA testing. This chapter cover the software used, the speckled pattern process, the calibration requirements, necessary equipment, and the setup that was followed for all tests carried out in this thesis.

2.1 Software Vic-3D

The DIC software Vic-3D and Vic-Gauge, developed by Correlated Solutions, Inc. was used in this study. Vic-3D provides a full-field 3-dimensional measurement of shape, displacement, and strain based on the principle of digital image correlation (Hild et al., 2006). DIC is an optical method that measures deformation on an object's surface. The method tracks the changes in gray value pattern in small neighborhoods called subsets during deformation (Hild et al., 2006). Essentially, Vic-3D works by taking pictures of a specimen being tested and comparing the deformed images to the reference image. The specimen is first prepared with a random speckled pattern (Figure 2.1) as will be discussed later. This pattern is what the software uses to create subsets. The software tracks the subsets in the deformed pictures and therefore calculates the displacements and strains. The subset size can be adjusted during the post-processing depending on the size of the speckled pattern.

Vic-3D has the capability of producing videos form the pictures taken during the test. These videos show the different colored contours of displacement and strain throughout the duration of the test. Data can also be exported at any desired point or slice on the specimen or it can be exported as the average of the speckled area, known as the area of interest (AOI).

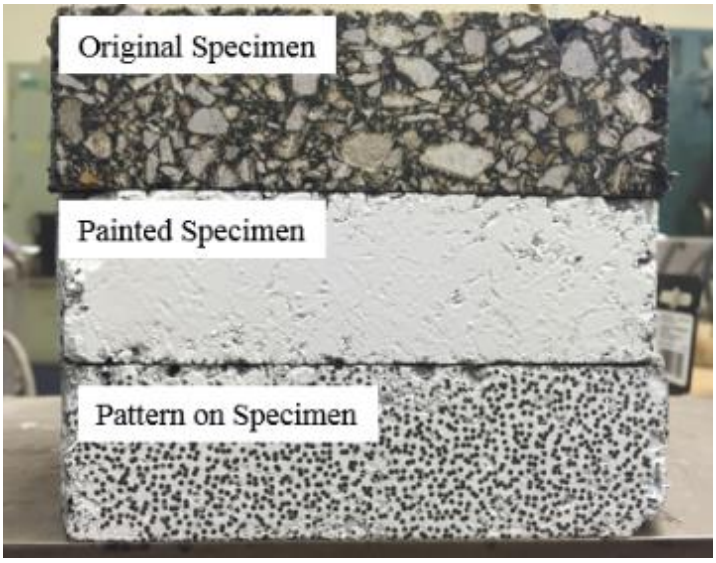

Figure 2.1: Specimen Preparation for DIC.

2.2 Speckle Pattern

The speckled pattern is a crucial aspect of DIC. The pattern has to be random and sized accordingly to the size of the object/specimen being tested (Figure 2.1). The pattern cannot be too large or the results will not be accurate. One of the challenges in this study was to develop the most efficient, repeatable, and useful way of applying the speckled patterns. First, the speckled pattern was applied by spraying paint directly from a spray can. This method was rapid and efficient yet it was difficult to control the size of the paint drops. Also, precise hand motion was needed to avoid leaving big black paint marks (Figure 2.2a). Another method used was creating a random pattern stencil in a computer numeric control (CNC) machine. The stencil was designed using Solid Works™ and was transferred to a 20-mil-thick steel plate. The stencil proved to work more effectively than the spray can. The drawback of the stencil was that the paint would smear by the time it dried (Figure 2.2c). The third method used was to transpose a random pattern that was created using the Speckle Generator from Correlated Solutions (Figure 2.2b). This was done by painting the specimen white and, once it dried, gluing the pattern using matte medium glue.

After about 15 minutes, the paper was gently rubbed with water and the ink of the pattern printed on the paper transposed to the specimen (Figure 2.3). For this study, the third option was chosen since it yielded the most defined pattern on the specimen.

The size of the speckled pattern has to be selected according to the size of the specimen. A pattern that is to large will not allow for enough point to be tracked in the deformed images and, therefore, the results will not be favorable. By trial and error, the speckled pattern between 0.04 in. and 0.05 in. in diameter yielded the best results for this type of specimen. The software divides the specimen into subsets based on the size of the pattern. The movement of each subset is then tracked during the post processing from photographs captured during the conduction of the test.

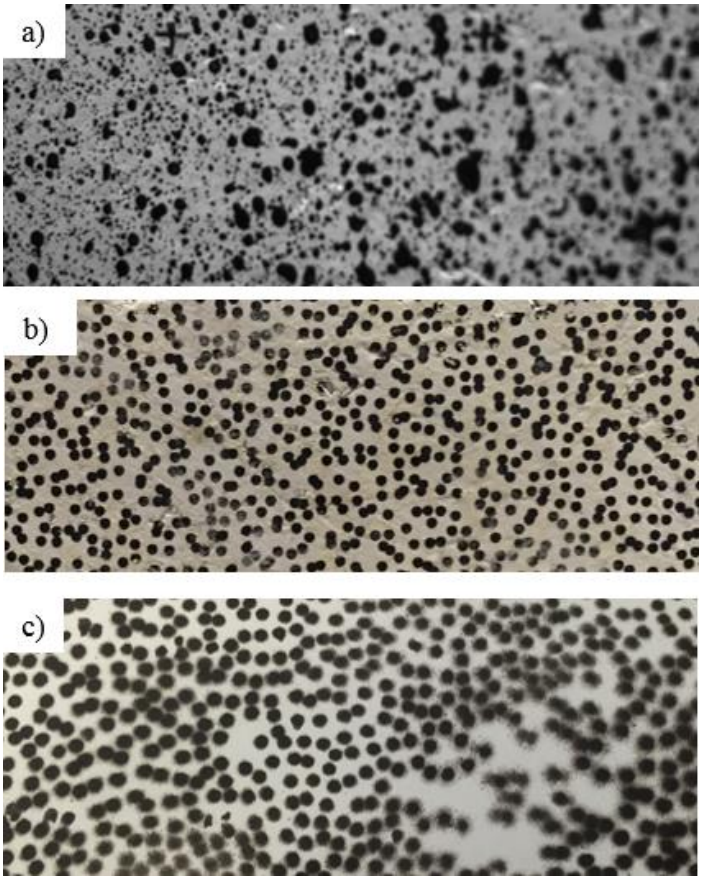

Figure 2.2: Different Speckle Patterns Tested. a) Spray Can b) Transpose c) Stencil

Figure 2.3: Speckle Pattern Application Process.

2.3 Calibration

The pictures need to be calibrated using a calibration card (Figure 2.4) that is included in the Vic-3D software package. The size of the calibration card has to be appropriate for the size of the speckled pattern as well as to the size of the object that is being tested. If the calibration card is too large a satisfactory calibration will not be reached. Even though it is recommended for the calibration card to cover most of the picture area, if a smaller calibration card is used, calibration can still be achieved. Approximately 20 photos of the calibration card in different positions and at slightly different angles have to be taken. These pictures are processed in the Vic-3D software so that the actual displacements and distances can be ascertained. If a satisfactory calibration is not reached, pictures of the calibration card have to be retaken. Another important factor in the calibration process is the amount of light present. If too much or too little light is used, a satisfactory calibration will not be reached. There has to be enough light to get clear and crisp images but not too much where it blurs the image (Figure 2.4a). Once calibration pictures are

processed the software gives a calibration score which is the overall error score, which is the standard deviation of residuals for all photos. According to Correlated Solutions a calibration with error of 0.05 and below is acceptable. Table 2.1 shows several of the scores obtained for different specimens.

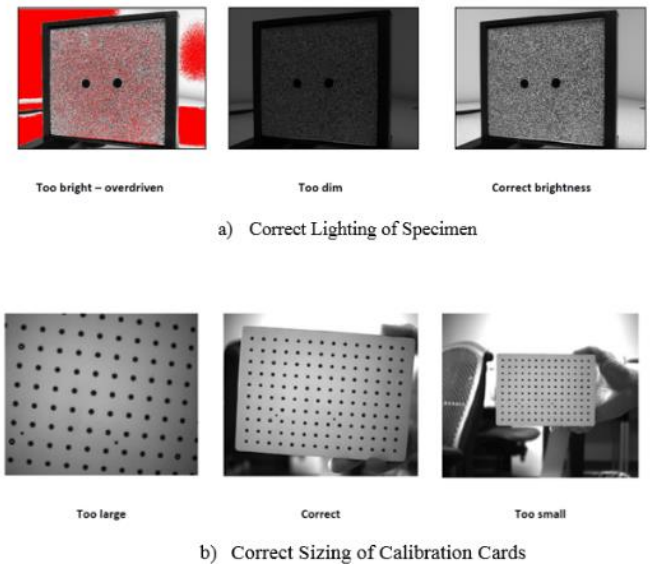

Figure 2.4: Key Aspects of DIC Setup Procedure

Table 2.1 Calibration Scores for Several Specimens

Specimen	**Calibration Score**
Specimen 1	0.012
Specimen 2	0.012
Specimen 3	0.011
Specimen 4	0.013
Specimen 5	0.011
Specimen 6	0.010
Specimen 7	0.012
Specimen 8	0.013
Specimen 10	0.012
Specimen 11	0.012
Specimen 12	0.012
Specimen 13	0.012

2.4 Equipment

The equipment necessary to run Vic-3D consists of two cameras, in this case, Point Grey GRAS-20S4M-C with 17-mm lenses, a tripod, and lights with controllable intensity (Figure 2.5). It is essential to use light sources with adjustable light intensity. Too much or too little light can impede a satisfactory calibration as will be explained below.

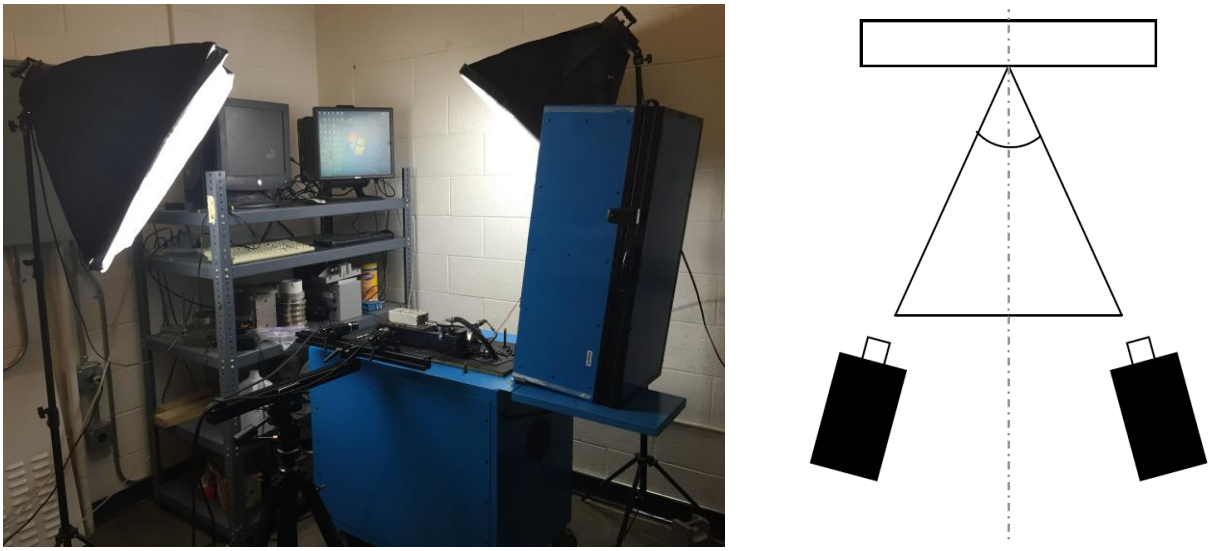

a) Equipment setup b) Angle between cameras

Figure 2.5: DIC System Setup.

Setting up the cameras is also an important step in the DIC process. The cameras have to be set up on a tripod and should be carefully and precisely leveled. Slightly inclined cameras can introduce significant errors in the results. The angle that is formed between the two cameras has to be adjusted according to the size of the lens of the camera (Figure 2.5b). In this case, since we used a 17-mm lens, the correct angle to use according to the Vic-3D manual is 25° or greater. During the setup, the light should also be positioned in a way that it brightens the image but that it does not directly shine onto the specimen. Once the tripod is leveled, the cameras are appropriately angled, and the proper lighting is selected, the setup cannot be changed in any shape for the

duration of the test including the calibration. It is important to perform the test with the same set up that was used for the calibration. If a different setup is used for the test, the calibration is no longer valid and therefore those results will not be accurate.

Chapter 3: Overlay Tester

The purpose of this study was to find out more information during the OT test than what the OT is able to show. This chapter describes the machine and the methodologies that are followed to glue and create the speckle pattern on the specimens. It also cover the results from the DIC analysis. This chapter also serves to validate the use of DIC in HMA testing through the use of the OT.

3.1 Device Characteristics and Specifications of OT Tests

Specification of the OT test procedure have been outlined in the Texas Department of Transportation (TxDOT) test procedure designation Tex-248-F. The OT is an electro-hydraulic system that applies tensile displacements to the HMA specimens. Figure 3.1 shows the main features of an OT specimen mounted on the plates that are used with the OT. One of the plates slides horizontally to simulate the opening and closing of the joints and/or existing cracks induced by tensile strains generated by vehicle loading and changes in temperature. The test can be conducted either cyclically or monotonically. During the cyclic tests, the specimen is repeatedly stretched by 0.025 in., every 10 seconds (one cycle), and back to its original position until the measured load decreases by 93% of the maximum peak load measured during the first cycle. During a monotonic test, the movable steel plate displaces once by 0.125 in. and returns back to its original position. An LVDT was added to the top of the specimen (Figure 3.1) to measure the displacement. This LVDT is not required by specifications but it was included to be able to gather more data from the test.

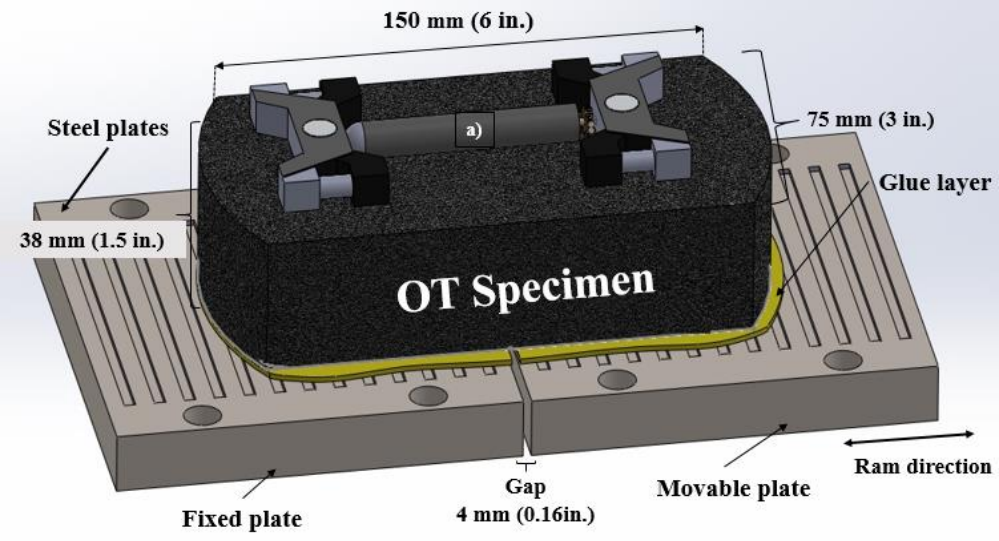

Figure 3.1: OT Schematic Layout

3.2 Gluing of Specimens

The gluing of the specimens onto the plates followed the methodology proposed by Garcia and Miramontes (2015). Figure 3.2 shows in detail step by step the process of gluing specimens. Figure 3.2a shows all the materials required to glue the specimens. First the plates are properly placed with a spacer (Figure 3.2b). Then a line is drawn at the center of the specimen and petroleum jelly and tape are placed to make sure there is no epoxy where the gap will be (Figure 3.2c-d). Equal amounts of epoxy, 8 grams, are place on each side and then the specimen is carefully centered to align with the plate gap and a 5-lb weigh is placed on top (Figure 3.2e-h). After the weigh is placed, excess glue is carefully cleaned and the tape and spacers are carefully removed (Figure 3.2h-l).

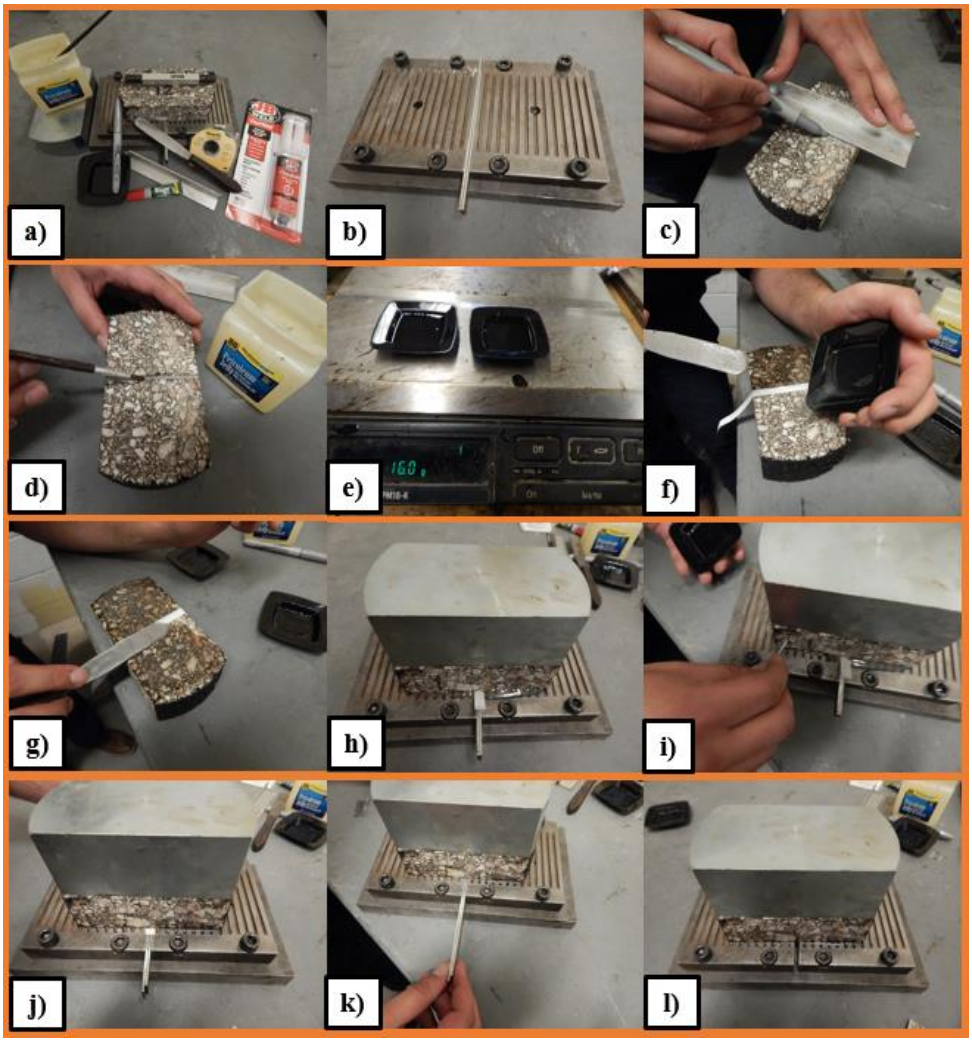

Figure 3.2: Steps of OT Specimen Preparation

3.3 Overlay Tester Results

In this section the results from the OT will be presented. The main purpose of this section is to verify that DIC can be applied to HMA testing and that the results recorded by the OT and LVDTs compare favorably.

3.3.1 Monotonic Condition

Figures 3.3 and 3.4 contain several displacement and strain frames during testing of the thin overlay mixture (TOM) under monotonic conditions. In the color spectrum, red represents the

greatest displacement/strain while violet represents the smallest displacement/strain. Figure 3.3-1 shows the unloaded displacement field before the OT test started. Figure 3.3-3, which shows the displacement pattern at the maximum displacement of the OT plate, demonstrates how negligible the displacement is on the left side (stationary side) of the specimen and the significant displacement that takes place on the right side (moving side). The red colors in the right-hand side signify the maximum deformation, while the violet color in the left side corresponds to the negligible movement of the specimen. The nonuniform displacement pattern within the specimen is evident. The maximum displacement for the monotonic condition is 0.125 in., the maximum displacement recorded by DIC was 0.128 in. The 0.003 in. difference can be considered as negligible since it is very small. Also the result from DIC is obtained from the movement of the visible face of the specimen while the 0.125 in. is the displacement of the plates.

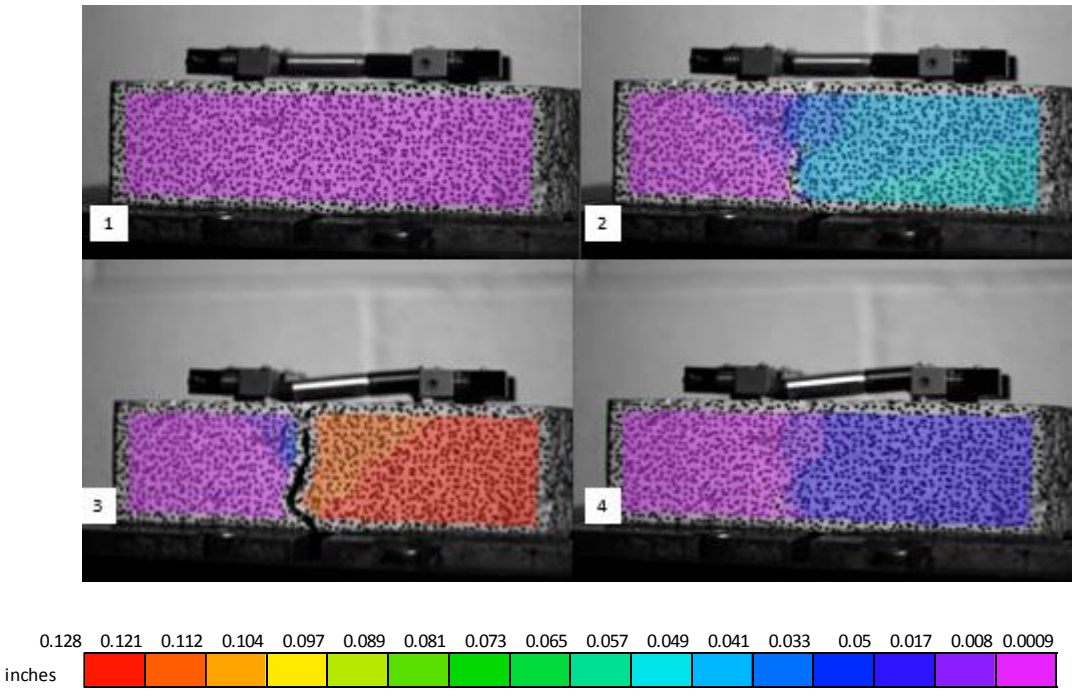

Figure 3.3: Monotonic OT DIC Displacement Results Specimen 10.

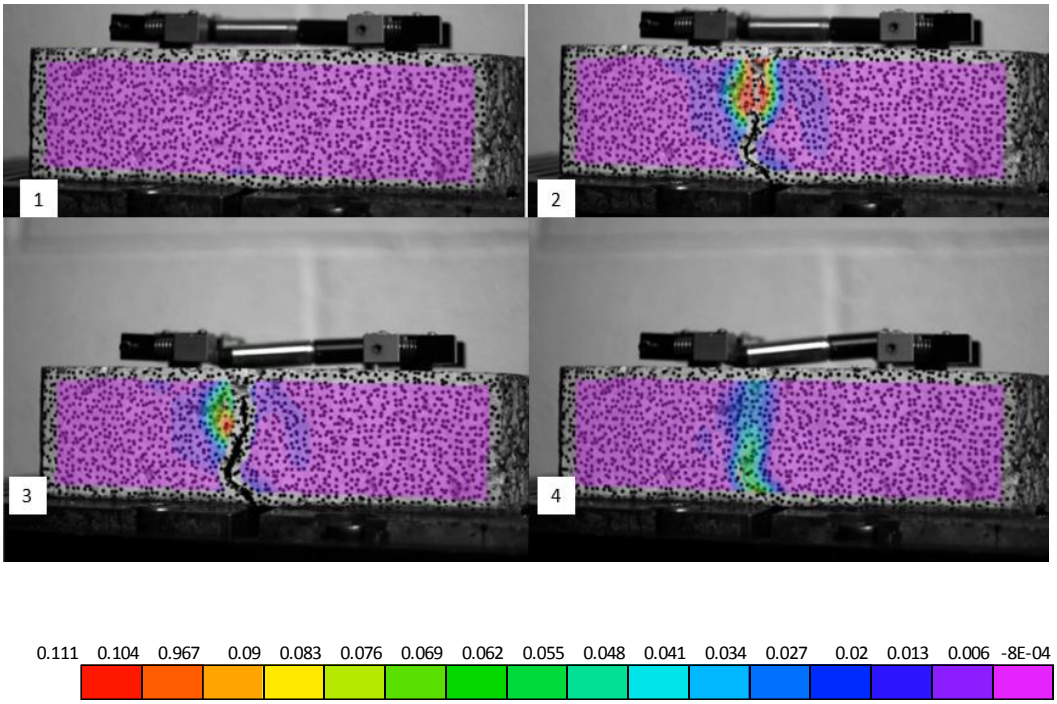

Figure 3.4: Monotonic OT DIC Strain Results Specimen 10.

Figure 3.4 shows the gradual evolution of the strain patterns during a monotonic OT test to failure. Figure 3.4-1 represents the strain field before the initiation of the test, while Figure 3.4-3 corresponds to when the maximum tensile displacement of 0.125 in. is applied. Figure 3.4-4 corresponds to the pushing of the plate back to home position (zero displacement). Almost all action is taking place along the plate gap where the crack initiates. Figure 3.5 shows the matrix of the aggregates and a close up of the crack of a TOM specimen. The crack development depends on the position of the aggregates and the crack will go around the larger size aggregates.

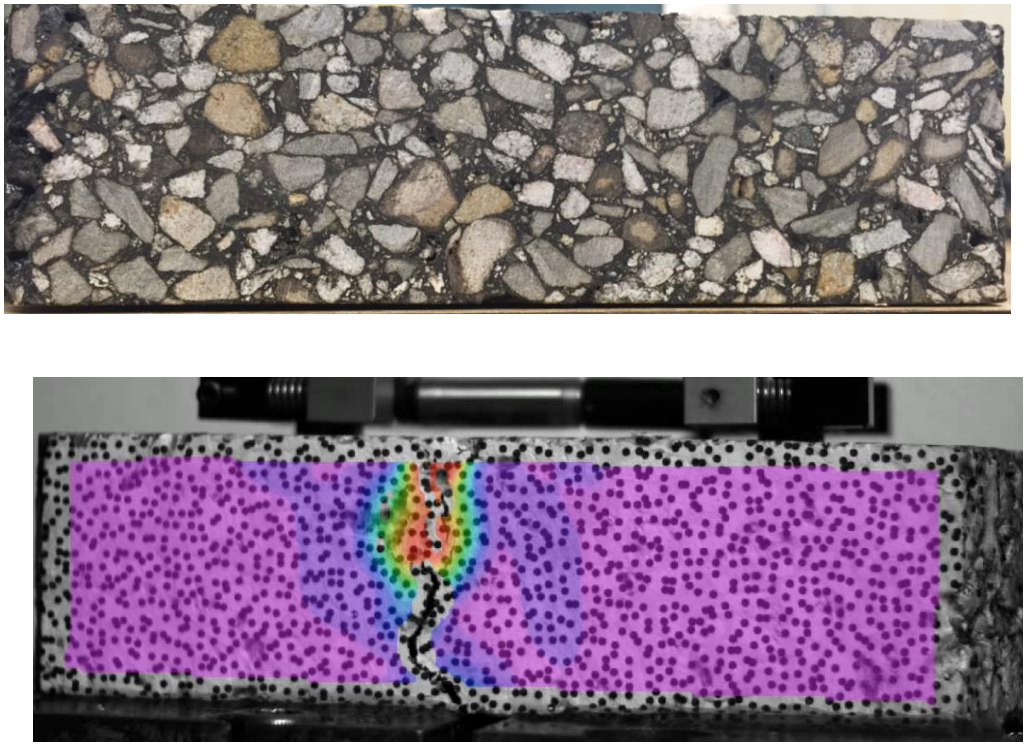

Figure 3.5: Aggregate Structure and Zoom In of Crack Specimen 10

Figures 3.6 through 3.8 represent the displacement time histories from the LVDT that is located on top of the specimen and the virtual LVDT from Vic-Gauge. The discrepancy in the start time of the two data acquisition systems results in the time difference between the results. The orange line which represents the top LVDT stops at around 15 seconds from the beginning of the test because the top LVDT snaps out of place at that time (Figure 3.4-3). The green line on Figure 3.9 corresponds to the virtual LVDT that was placed on the specimen using Vic-Gauge. With the physical LVDT approximately only 15 seconds of the test data was acquired while with the virtual LVDT it was possible to acquire data for the duration of the complete test. The data among the three different specimens of a TOM mix is consistent. The peak displacements in Figures 3.6 through 3.8 are practically the same on all three specimens (0.115 in., 0.115 in., and 0.116 in., respectively). These graphs serve as another reinforcement for the use of DIC in asphalt testing.

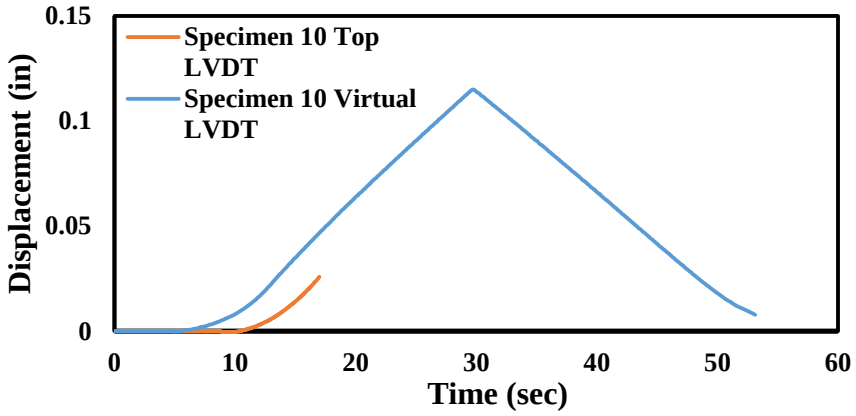

Figure 3.6: Monotonic Displacement of Specimen 10

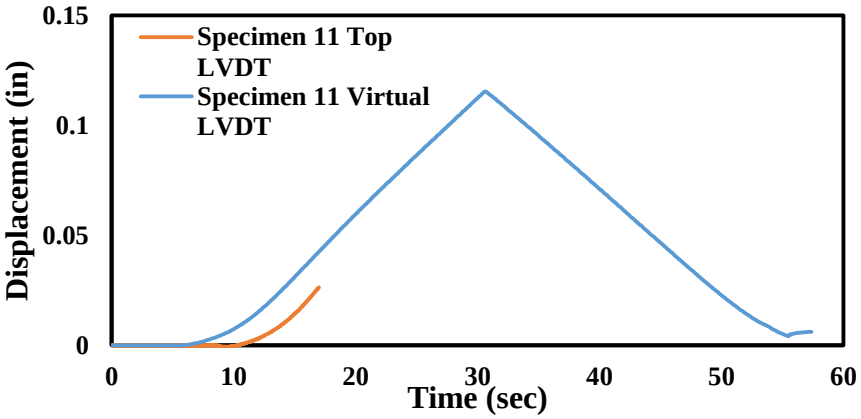

Figure 3.7 Monotonic Displacement of Specimen 11

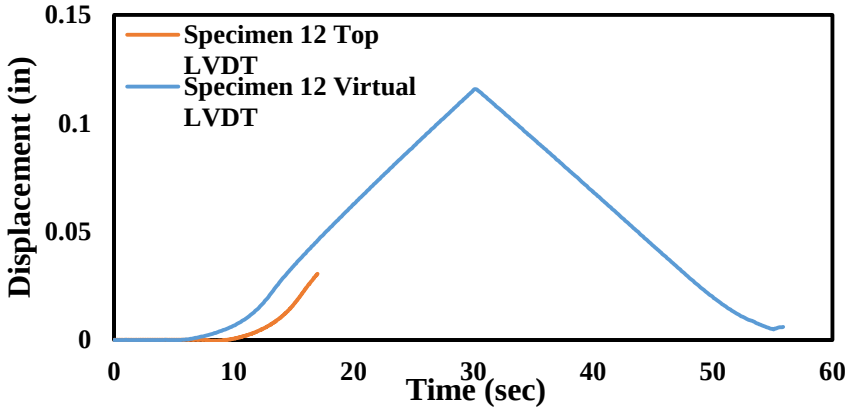

Figure 3.8: Monotonic Displacement of Specimen 12

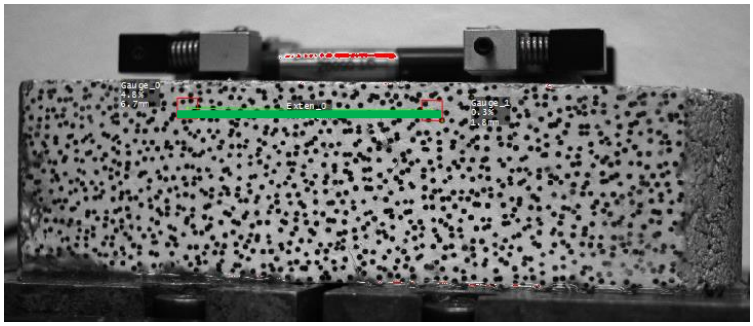

Figure 3.9: Virtual Extensometer Location for OT

3.3.2 Cyclic Condition

The OT specimens under the cyclic condition behave similar to the monotonic tests in that most of the deformation also takes place in the center of the specimen close to the plate gap. Figures 3.10 and 3.11 show several frames during a cyclic OT test of TOM mix. Figure 3.10-1 represents the beginning of the cycle and Figure 3.10-2 corresponds to the results at the maximum plate opening of 0.025 in. Figures 3.10-3 and 3.10.-4 correspond to the data as the plate is pushed back to the home position. The displacement scale on Figure 3.10, with a maximum displacement of 0.026 in., demonstrates the accuracy of DIC, since we know that the plates open to a maximum distance of 0.025in.

After the first cycle the calculation of strain with the LVDT is unattainable. The use of DIC can provide the strain information of the specimen. Even though we cannot compare the results to actual data, it can be assumed that the strains are correct given that the displacements have already been corroborated. Figure 3.6 shows the strain fields during one cycle of the test with part 2 being at the maximum displacement of the plates.

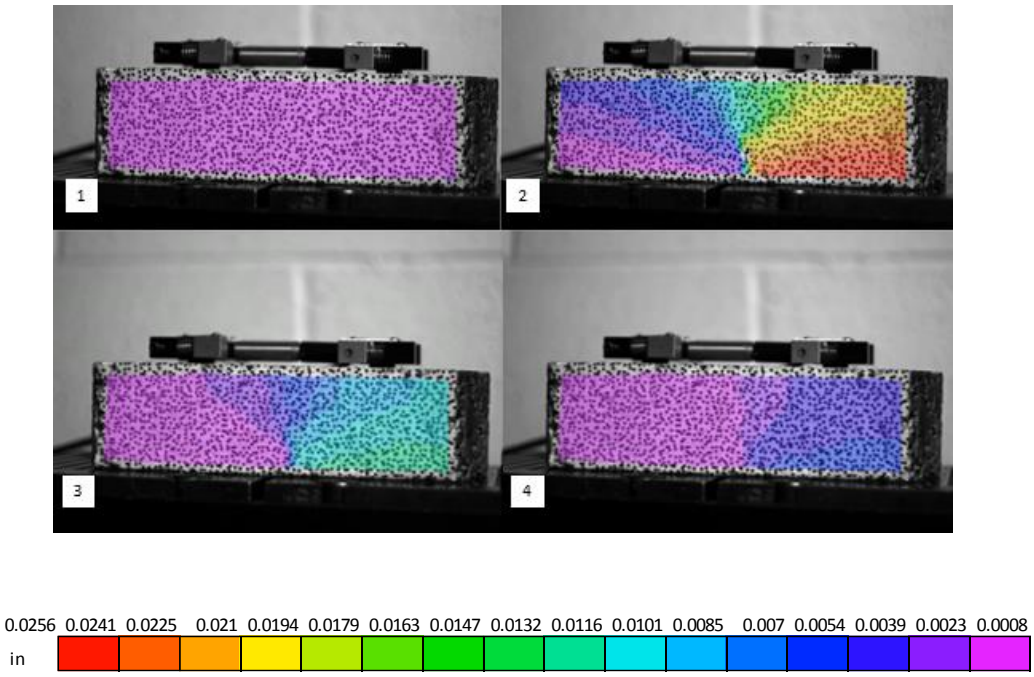

Figure 3.10: Cyclic OT DIC Displacement Results Specimen 3.

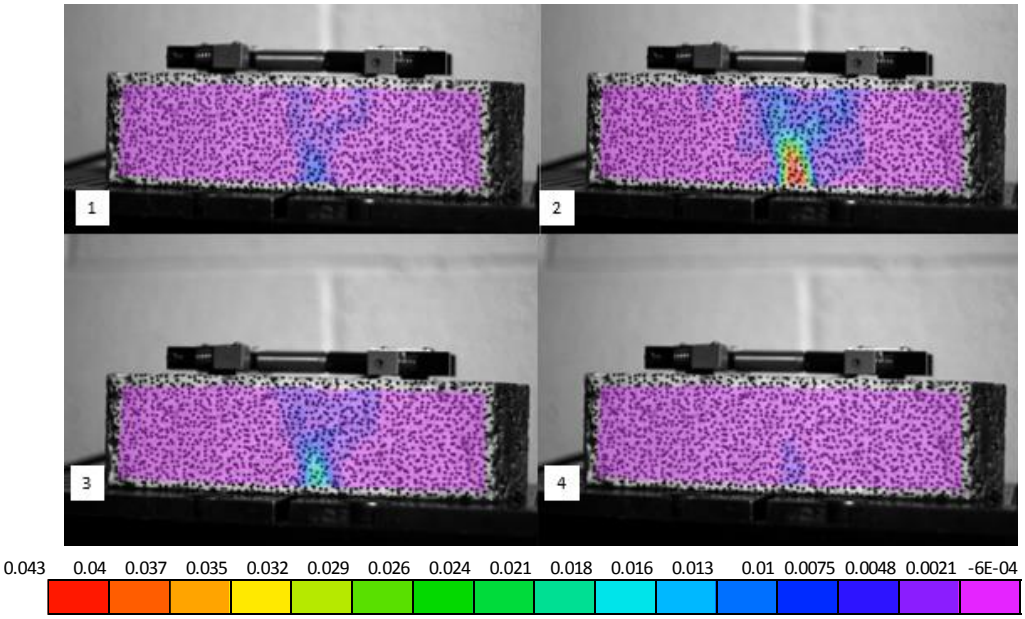

Figure 3.11: Cyclic OT DIC Strain Results Specimen 3.

Figures 3.12 through 3.14 show the displacement time histories of the on-specimen LVDT and virtual LVDT for a cyclic OT test. Once again, there is a discrepancy between the start times of the two systems. As with the monotonic tests, the cyclic tests are consistent with one other.

Specimen 3, Figure 3.14, is of special significance. Both curves, one which represents the physical LVDT and the other which represents the virtual LVDT are almost on top of one another. It should be pointed out that it cannot be expected to have the exact same curves since the physical LVDT is collecting data from the top of the specimen, while the virtual LVDT is collecting data from the front face of the specimen.

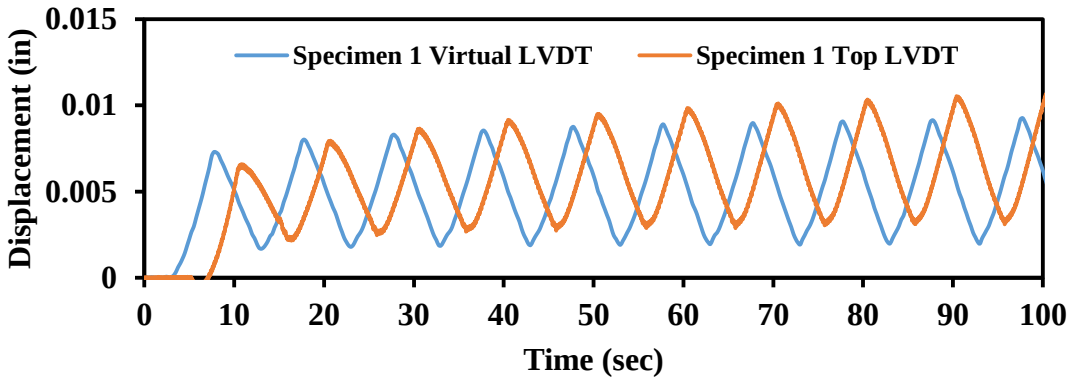

Figure 3.12: Cyclic Displacement of Specimen 1

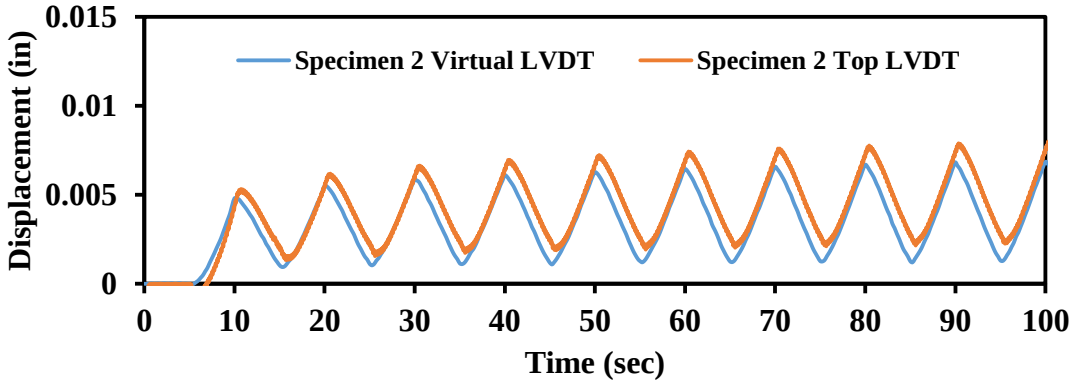

Figure 3.13: Cyclic Displacement of Specimen 2

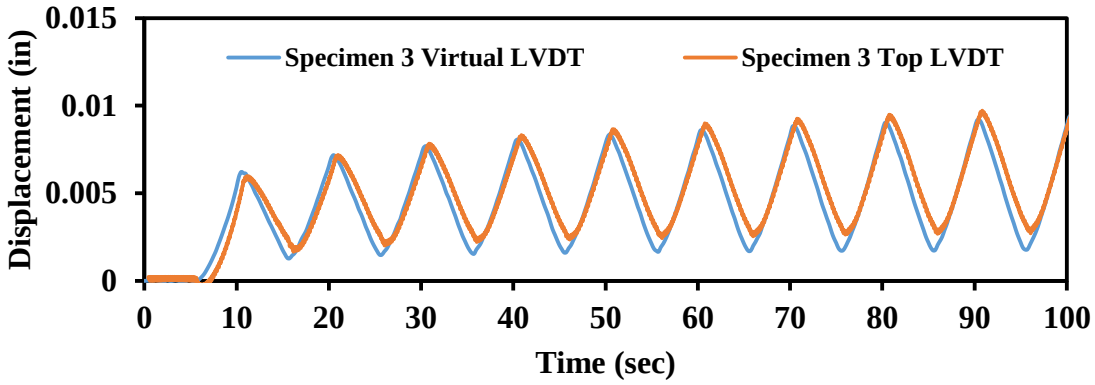

Figure 3.14: Cyclic Displacement of Specimen 3

Appendix A contains the results of the rest of the OT specimens for SPD and Type D materials. There is also a discrepancy with the start times as with the TOM specimens. Overall it appears that the use of DIC is favorable in the OT Test.

Chapter 4: Indirect Tensile Test

The purpose of this chapter is to introduce the IDT test specifications and to present the results from the use of DIC for this testing method. The use of DIC in this test shows its versatility. Since IDT test is performed at a much faster loading rate than OT, it shows that DIC also works with faster paced tests.

4.1 Specifications

The IDT test were performed following ASTM D693, "Standard Test Method for Indirect Tensile (IDT) Strength of Bituminous Mixtures." The specimens had a diameter of 4 inches. The specimens were conditioned to a temperature of 77°F before the tests were performed. The loading rate for this test was 1.97 in/min. Three specimens of the three mixes explained in Table 1.2 were tested. The tests were conducted in an environmental chamber to make sure the temperature was consistent during test.

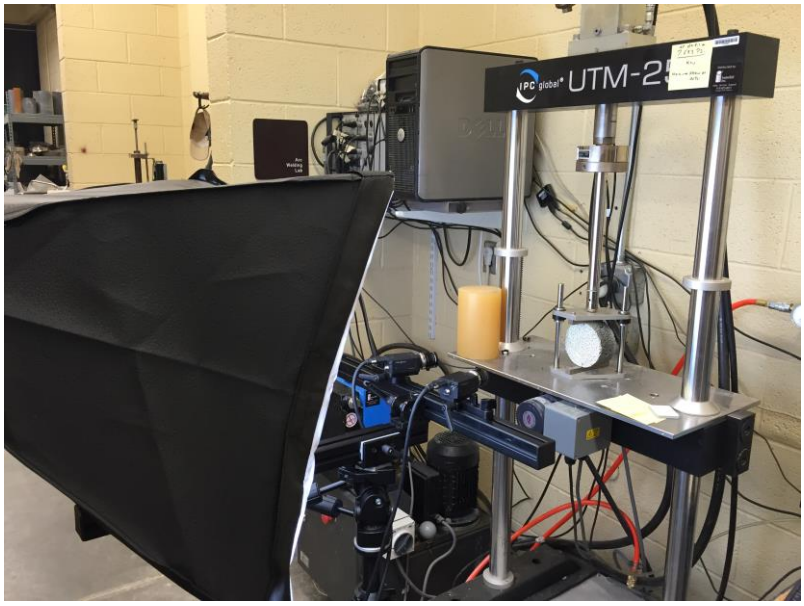

Figure 4.1: IDT Machine Setup

4.2 IDT Results

Figures 4.2 and 4.3 show the displacement and strain frames of an IDT test, respectively. As expected, the strain concentration happens under where the load is being applied. As with the OT test, it was simple to develop the contours in Figures 4.2 and 4.3 using Vic-3D. The only difference was that with the IDT test there was less amount of information (pictures) since the test is carried out so rapidly.

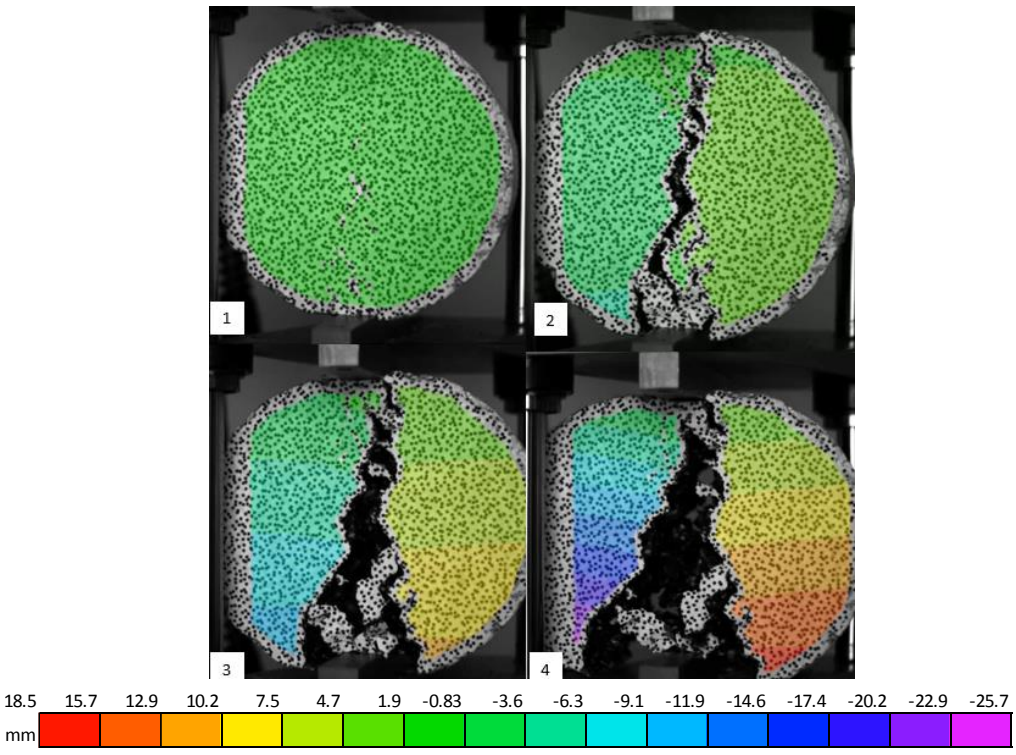

Figure 4.2: IDT DIC Displacement Results Specimen 28.

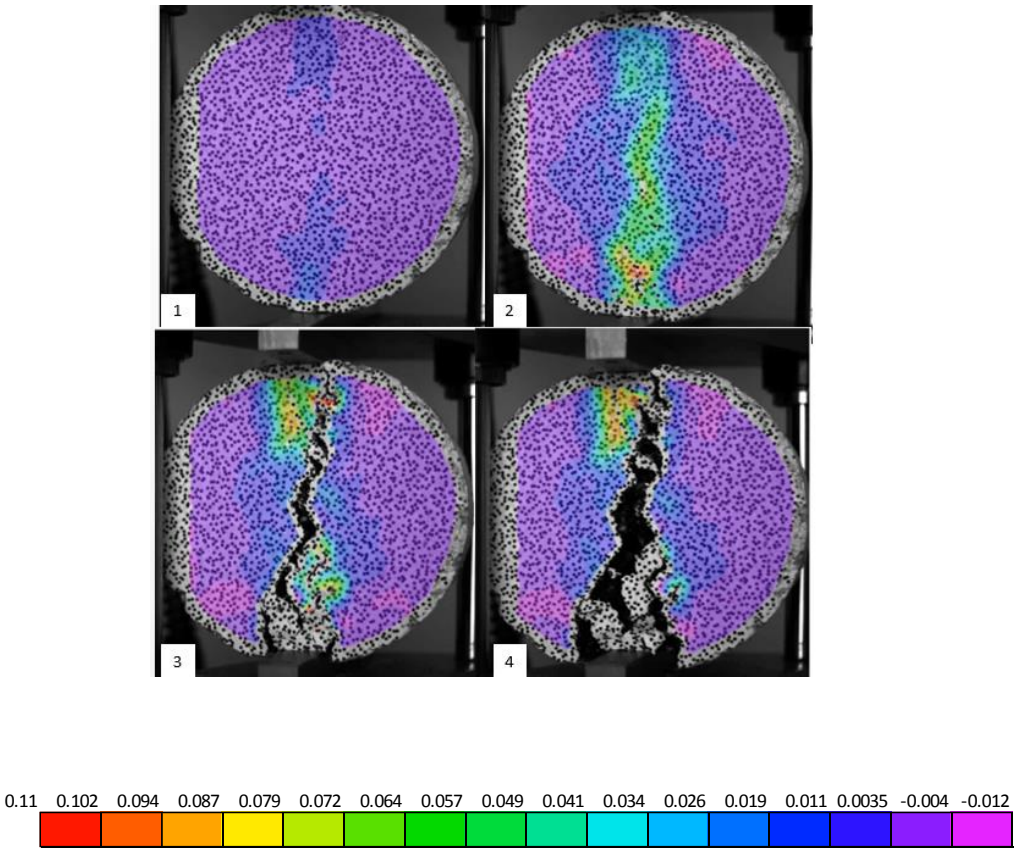

Figure 4.3: IDT DIC Strain Results Specimen 28.

Table 4.1 shows the maximum strains for the specimens of the different mixes tested. All of the values are within range of each other. This values show consistency between the tests, about a 10% difference between each other and all mixes have a relatively low .

Table 4.1 Max Strain for IDT Specimens

Material	Specimen	Max Strain (in/in)	Average	Std Dev	COV
TOM	28	0.11	0.108	0.009	8%
	29	0.116			
	30	0.099			
SPD	31	0.110	0.113	0.019	17%
	32	0.133			
	33	0.096			
Type D	34	0.119	0.111	0.007	6%
	35	0.105			
	36	0.109			

A virtual LVDT was placed horizontally on the middle of each specimen. Figure 4.4 shows the results for the SPD, TOM, and Type D mixes. It should be noted the time was adjusted on all tests to account for discrepancies due to start times of the different machines. On Figure 4.4 the average of the five test was plotted and with one standard deviation. It appears from Figure 4.4 that the mix with the greatest variability is Type D, while the one with the least is SPD.

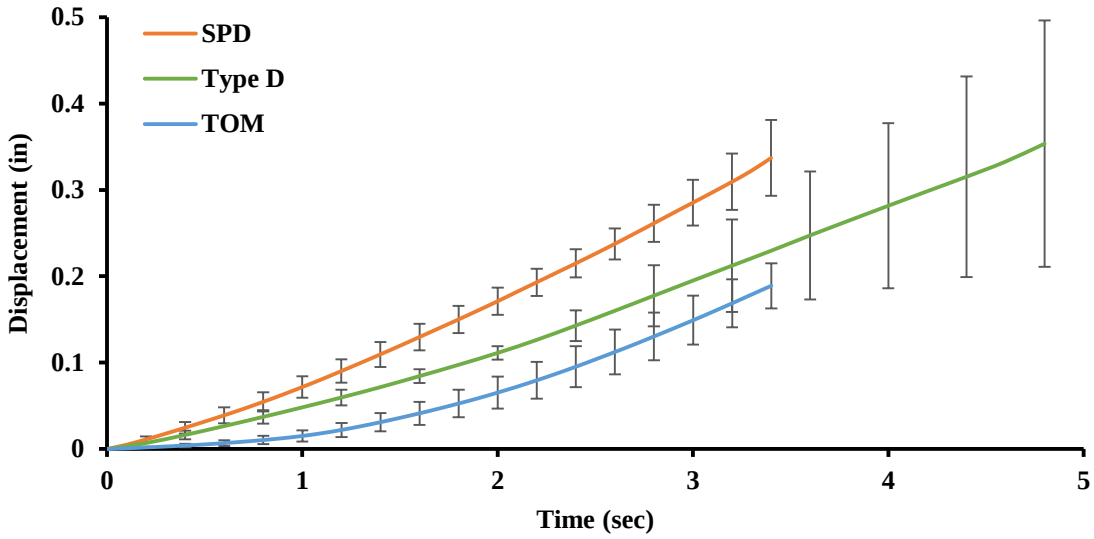

Figure 4.4: IDT Average Results

The use of DIC with the IDT test also demonstrated that the test has to be carried out very cautiously. For this thesis all IDT tests had to be performed twice because after the post processing of the DIC it was clearly seen on the videos that if the specimen was not accurately centered one side of the specimen would be loaded more than the other side or that there was a visible rotation of the specimen. The use of DIC can be beneficial to the industry because through its use issues related to a test can be determined, that otherwise would go unperceived.

Chapter 5: Semi-Circular Bending Test

5.1 Specifications

The SCB testing set up is illustrated in Figure 5.1. The SCB test specimens were compacted to a nominal air void content of 7% ± 1. The specimens are obtained by cutting 2 inches from the center of the compacted cylinder. Different notch depths were used for this study. The nominal notch depths were 0.94 in., 1.18 in., and 1.42 in. The load rate for the SCB test is 0.0197 in/min at a temperature of 77°F. The SCB tests were also conducted in an environmental chamber to maintain the temperature constant throughout the tests. The process to apply the speckled pattern on the SCB specimens was the same as the one followed for the OT specimens.

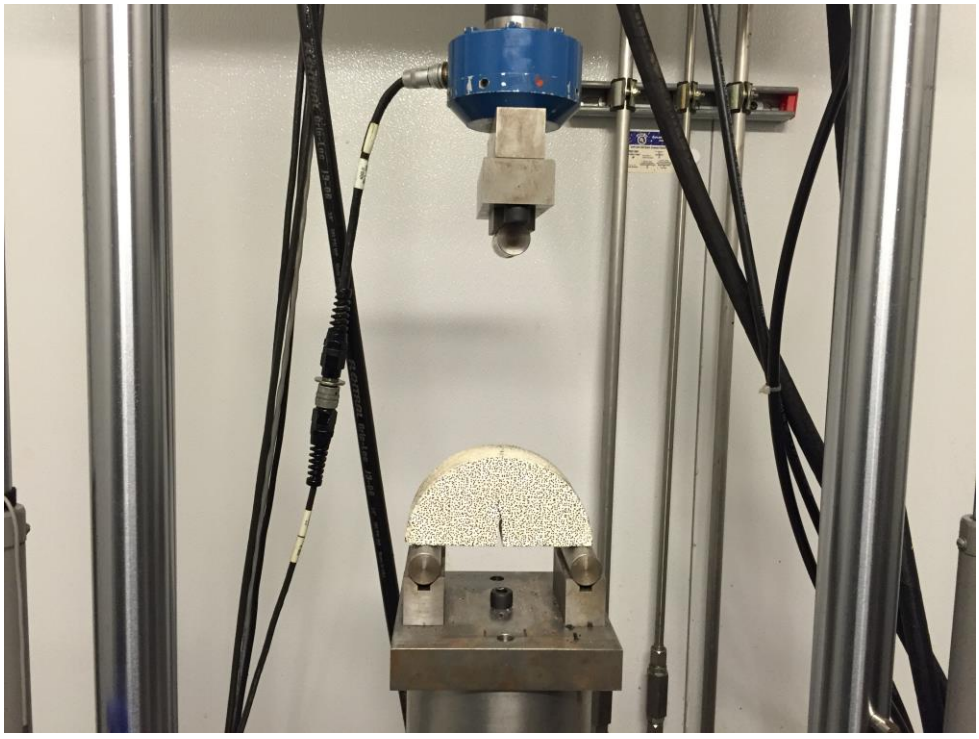

Figure 5.1: SCB Setup

5.2 SCB Results

Figures 5.2 and 5.3 are frames from the displacement and strain fields of an SCB test, respectively. In Figure 5.2, the purple end of the scale is negative while the red end is positive. In Figure 5.2-4 this means that one side of the specimen is moving to the left as the other side is moving to the right at the same rate.

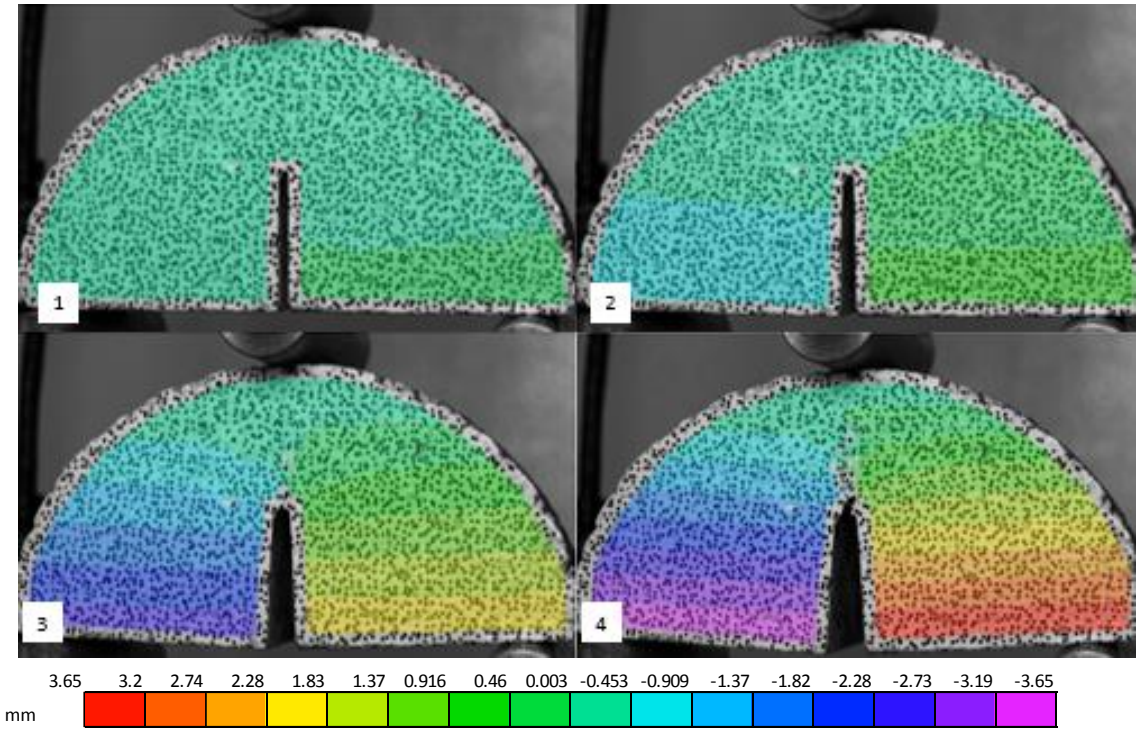

Figure 5.2: SCB DIC Displacement Results Specimen 21.

Figure 5.3 represents the strain field of the same specimen as in Figure 5.2. Part one of Figure 5.3 is right at the beginning of the test, while part 4 is right at the end once the specimen has already failed. The strain concentration occurs right under the load and immediately above the notch, the rest of the specimen is practically undisturbed.

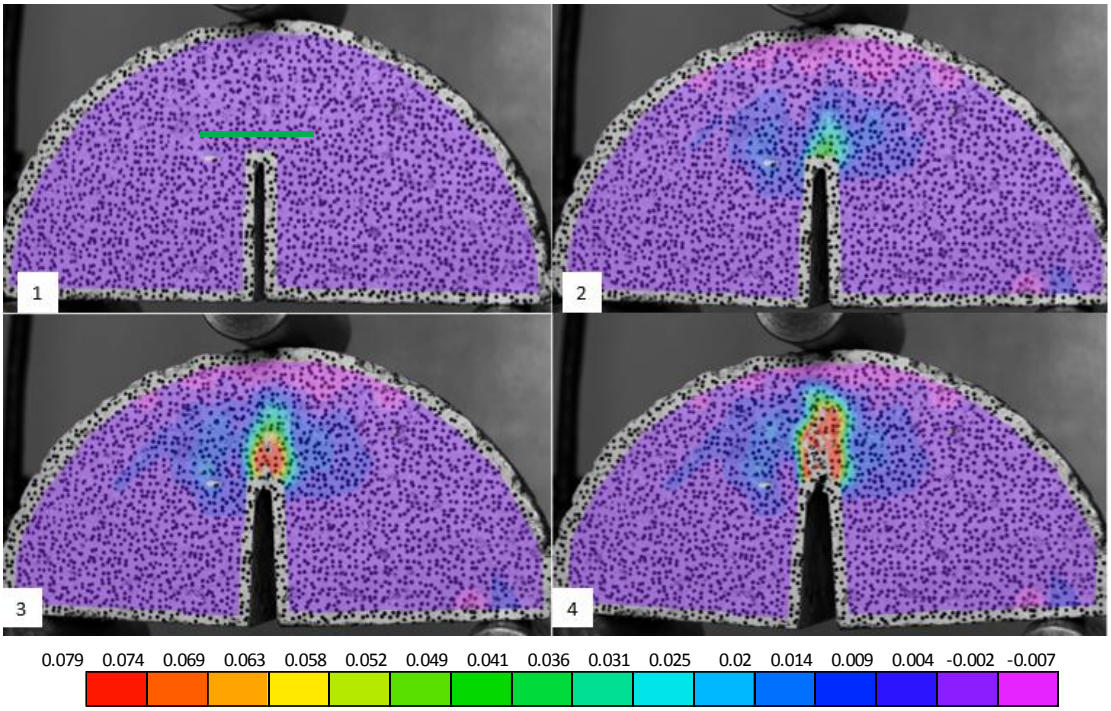

Figure 5.3: SCB DIC Strain Results Specimen 21.

A virtual gauge, using Vic-Gauge, was placed on every specimen right above the notch. With the information obtained from that virtual LVDT displacement time history was obtained. Figures 5.4, 5.5 and 5.6 are representative of the load time histories for the three different materials used in this study. The dash line represents the displacement while the solid line represents the load.

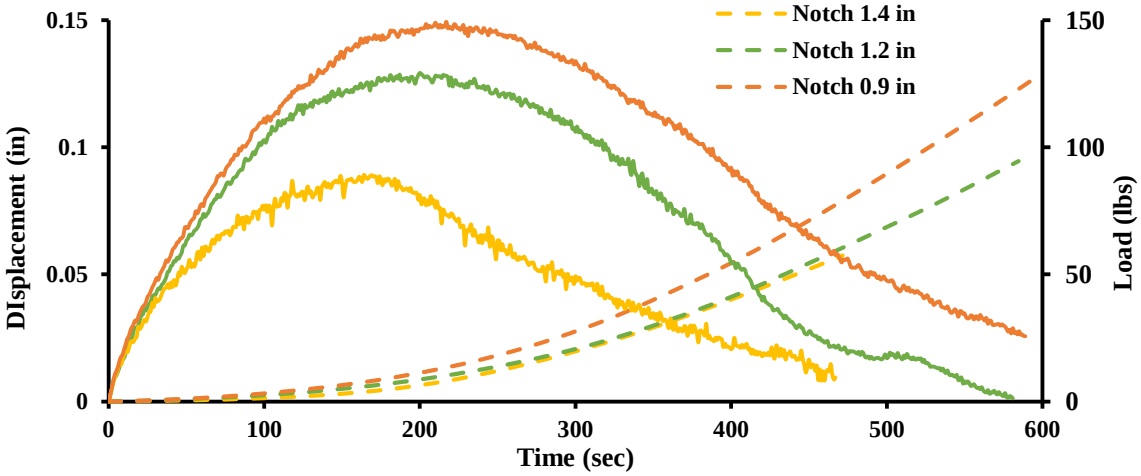

Figure 5.4: Load and Displacement Time Histories for TOM Mixes

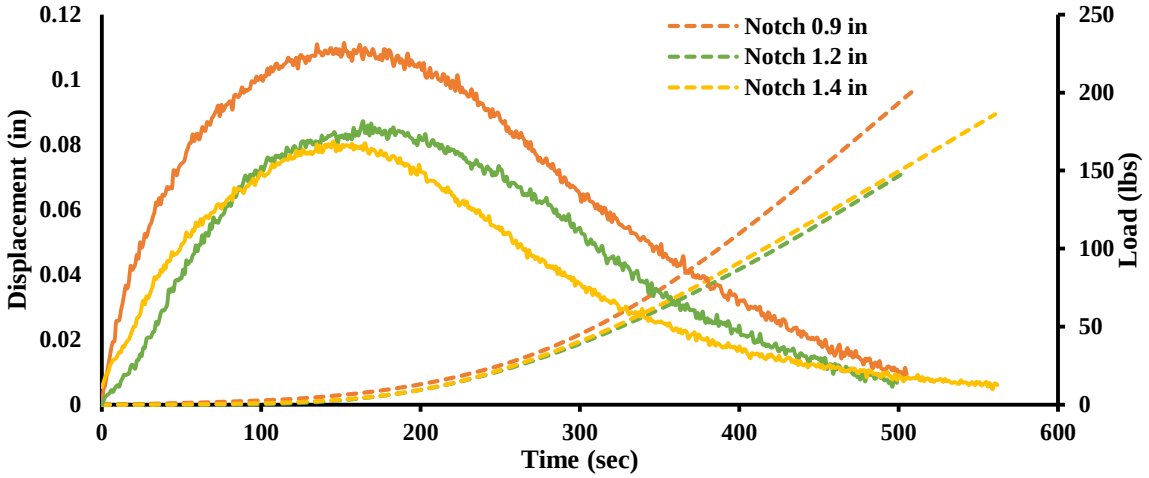

Figure 5.5: Load and Displacement Time Histories for SPD Mixes

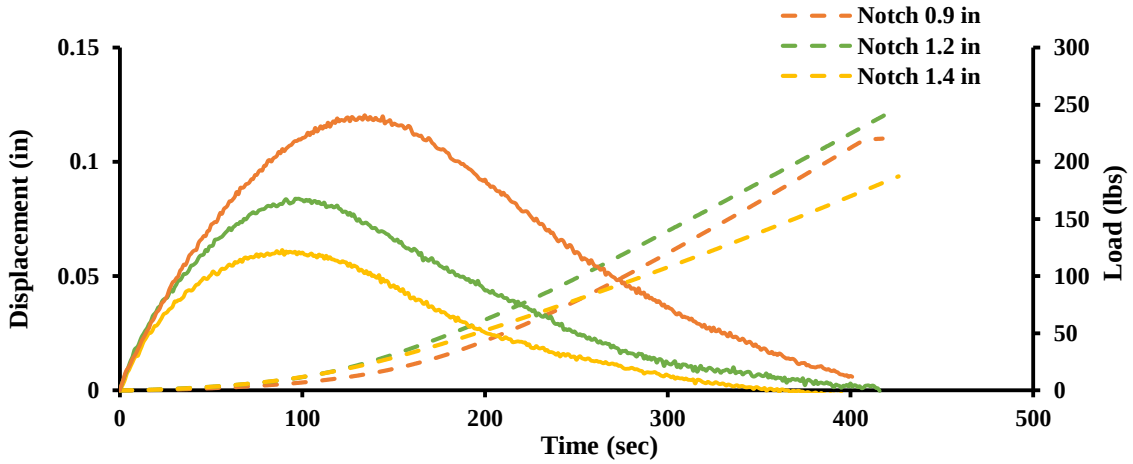

Figure 5.6: Load and Displacement Time Histories for Type D Mixes

Figures 5.7-5.9 show a close up of the first 200 seconds of Figure 5.5. From the three graphs (Figures 5.7-5.9) the same pattern can be detected. As the load increases up to where it reaches the peak load, the displacement increases almost in a linearly way. Once the load has reached it maximum peak the displacement begins to grow exponentially. It can be said from the figures that once the test had reached its maximum load the displacement follows no certain path. Specimen 22, which has the smallest notch, 24mm,

is the specimen that requires the greatest load to fail and therefore produces the greatest displacement. The difference in displacements between the three specimens is another indication that the DIC results are correct since it would be expected to have a greater displacement with the smallest notch and a smaller displacement with the greatest notch.

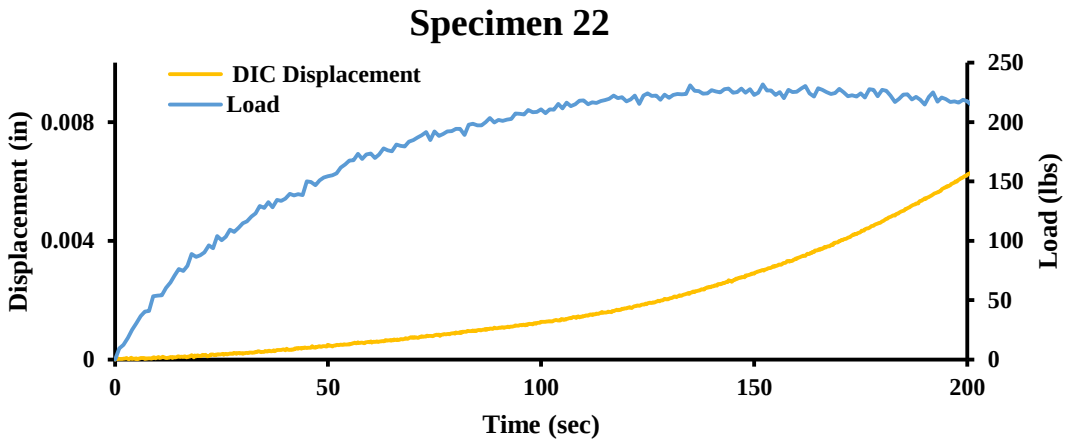

Figure 5.7: Load and Displacement - Specimen 22

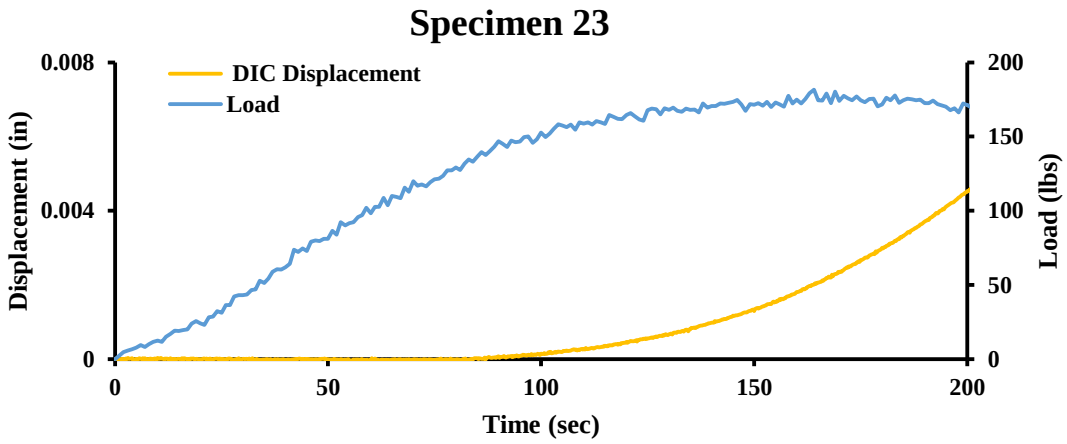

Figure 5.8: Load and Displacement - Specimen 23

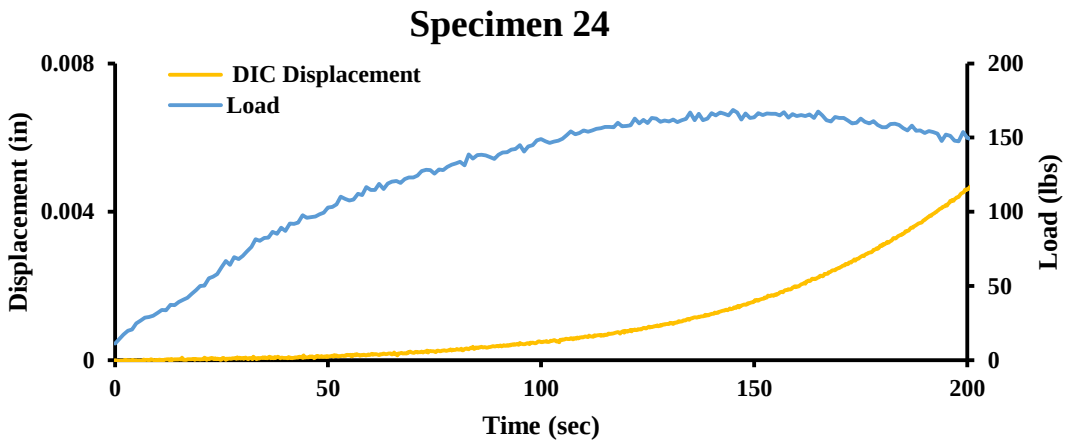

Figure 5.9: Load and Displacement - Specimen 24

Chapter 6: Summary, Conclusion, and Recommendations

6.1 Summary

The objective of this study was to develop a methodology for the use of DIC as an alternative measuring technique for HMA. This study was focused on how to prepare the specimen and the setup of the system, including lighting and calibration and to validate the results obtained through DIC. From this study it is recommended that the technique used for the speckle pattern be by the transpose method.

Through the use of three different HMA tests it was shown that DIC data compares very favorably with data from the test machines. DIC serves as a good alternative to gather more information and to know more about a test. The advantages of DIC are as follows:

- It is a noncontact measuring technique
- Results are comparable to those measured with contact traditional sensors
- Measurements can be carried out at more than one location
- Videos can be created that show the stress and strain fields in a color spectrum
- Helps predict crack path and initiation
- Can obtain different parameters from one test (displacements, strains, etc.)
- Data can be acquired throughout the duration of the test, as shown by the OT monotonic test

The use of the DIC was helpful in understanding better the behavior of a specimen during the different tests presented in this thesis. The following are conclusions that can be made based on the DIC analysis for each test:

Overlay Tester

- Negligible movements within the specimen were observed on the portion of the specimen that was glued to the stationary OT plate.
- The location and the orientation of the crack can be predicted before the crack fully propagates by the color contours developed through DIC.
- The strain field is fully concentrated at the center of the specimen near the plate gap.
- Given that the displacements obtained using the DIC are close to those from the OT device, it can be concluded that the strains from the DIC system are also close to the actual strains.

Indirect Tensile Test

- The IDT test has to be very cautiously set up to avoid the specimen from moving during the test.
- The fast loading rate of the IDT test shows the versatile of the DIC technique since it can be used in both slower load rate, such as the SCB test and in faster rates.

Semicircular Bending Test

- As with the OT, all the strain concentrates in one area, right above the notch.
- The displacement has follows a linear path until it reaches the maximum load is reached, once the maximum load is reached, the displacement begins to grow exponentially.
- Once the load is being applied half of the specimen moves to one side while the other half moves equally in the other direction.

6.2 Conclusions

Traditional measuring devices such as LVDTs and gauges are widely used for data acquisition in asphalt testing. Lately it has become an area of interest on how accurate and reliable this measuring devices are. This thesis shows a novel way of using technology as an alternative

solution. Through the results present here it has been concluded that DIC can be used reliably as a measuring device or in conjunction with other traditional devices.

6.3 Recommendations

The recommendations of this study for future work include further research on how to use the all the data can be acquired through the use of DIC. The main purpose of this thesis was to validate the use of DIC in HMA testing. Now that it has been demonstrated that the data acquired is consistent with results obtained through these test, it is recommended for further exploration on other parameters that can be obtained from DIC, such as the change in Poisson Ratio that can be obtained from the strain in X and Y directions and the shear stress. It is also recommended to develop an approach to be able to coordinate systems to start and end simultaneously to avoid any time misinterpretations. Lastly since this thesis focused on asphalt it is recommended to begin testing in soils to validate if DIC can also be used for these types of tests.

References

1. Aragao, F. T. S., & Kim, Y. R. (2011). "Characterization of Fracture Properties of Asphalt Mixtures Based on Cohesive Zone Modeling and Digital Image Correlation Technique." In Transportation Research Board 90th Annual Meeting (No. 11-1229).

2. Bennert, T. and Ali, M. (2008). "Field and Laboratory Evaluation of a Reflective Crack Interlayer in New Jersey," Transportation Research Board.

3. Bennert, T., Worden, M., and Turo, M. (2009). "Field and Laboratory Forensic Analysis of Reflective Cracking on Massachusetts Interstate 495." Transportation Research Board.

4. Chehab, G. R., Seo Y., and Kim Y. R. (2007) "Viscoelastoplastic Damage Characterization of Asphalt–Aggregate Mixtures Using Digital Image Correlation." International Journal of Geomechanics, Vol. 7, No. 2, pp. 111–118.

5. Choi, S., and Shah, S. P., (1997) "Measurement of Deformations on Concrete Subjected to Compression Using Image Correlation." Experimental Mechanics, Vol. 37, No. 3.

6. Chong, K., & Kuruppu, M. D. (1984). "New Specimen for Fracture Toughness Determination for Tock and Other Materials." International Journal of Fracture, 26(2), R59-R62.

7. Daniel, J. S., Chehab, G. R., and Kim, Y. R. (2004). "Issues affecting measurement of the complex modulus of asphalt concrete." Journal of materials in civil engineering, 16(5), 469-476.

8. Gao, G., Huang, S., Xia, K., and Li, Z. (2014). "Application of Digital Image Correlation (DIC) in Dynamic Notched Semi-Circular Bend (NSCB) Tests." Experimental Mechanics, 55(1), 95-104.

9. Garcia, V. and A. Miramontes. (2015) "Understanding Sources of Variability of Overlay Test Procedure." Transportation Research Record: Journal of the Transportation Research Board, No. 2507, pp. 10-18, Washington, D.C.

10. Germann, F. P. and Lytton, R. L. (1979). "Methodology for Predicting the Reflection Cracking Life of Asphalt Concrete Overlays." Research Report FHWA/TX-79/09+207-5.

11. Hajj, E., Sebaaly, P., Porras, J., and Azofeifa, J. (2010). "Reflective Cracking of Flexible Pavements Phase III: Field Verification." Research Report No. 13KJ-1, Nevada Department of Transportation, Research Division, University of Nevada, Reno.

12. Hild, F., and Roux, S. (2006) "Measuring Stress Intensity Factors with a Camera: Integrated Digital Image Correlation (I-DIC)." Comptes Rendus Mécanique, Vol. 334, No. 1, pp. 8–12.

13. Kim, Y. R., and Wen, H. (2002). “Fracture Energy from Indirect Tension Testing.” Asphalt Paving Technology, 71, 779-793.

14. Laurin, F., Charrier, J.-S., Lévêque, D., Maire, J.-F., Mavel, A., and Nuñez, P. (2012) “Determination of the Properties of Composite Materials Thanks to Digital Image Correlation Measurements.” Procedia IUTAM, Vol. 4, No. 0, pp. 106–115.

15. Seo, Y., Kim, Y., Witczak, M., and Bonaquist, R. (2002). “Application of Digital Image Correlation Method to Mechanical Testing of Asphalt-Aggregate Mixtures.” Transportation Research Record: Journal of the Transportation Research Board, (1789) 162-172.

16. Walubita, L. F., Faruk, A. N., Koohi, Y., Luo, R., and Scullion, T. (2013). “The Overlay Tester (OT): Comparison with Other Crack Test Methods and Recommendations for Surrogate Crack Tests.” 7(2), 180.

17. Walubita, Lubinda F; Faruk, A. N. (2012). “The Overlay Tester: A Sensitivity Study to Improve Repeatability and Minimize Variability in the Test Results.” 7(2).

18. Yi-Qiu, T., Lei, Z., Meng, G., and Li-Yan, S. (2012) “Investigation of the Deformation Properties of Asphalt Mixtures with DIC Technique.” Construction and Building Materials, Vol. 37, 2012, pp. 581–590.

19. Zhou, F., and Scullion T. (2013) “Upgraded Overlay Tester and Its Application to Characterize Reflection Cracking Resistance of Asphalt Mixtures.” Report No. FHWA/TX-04/0-4467-1, TTI.

Appendix A

Appendix A contains the reaming graphs showing the results from the different mixes.

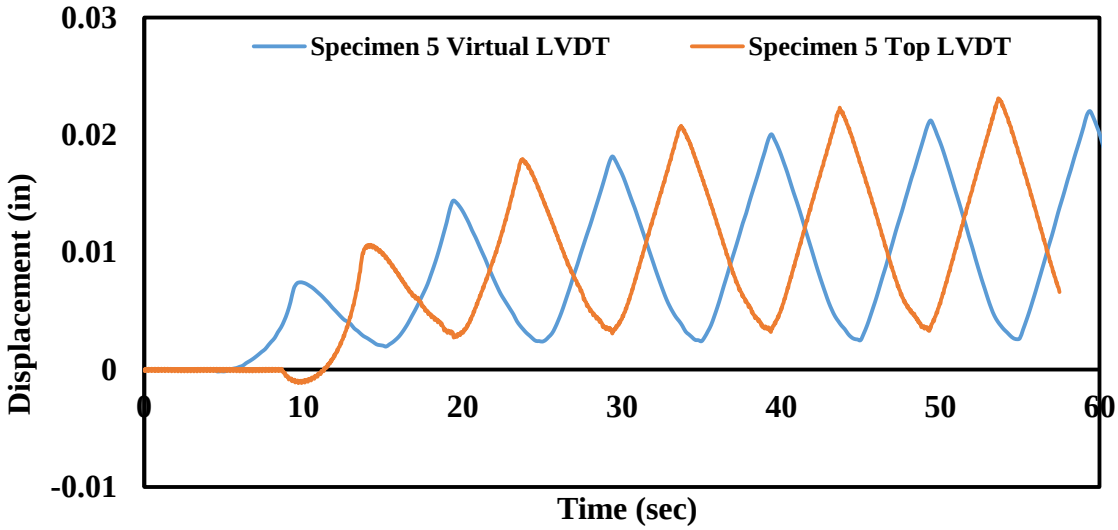

Figure A1 Cyclic Displacement of Specimen 5

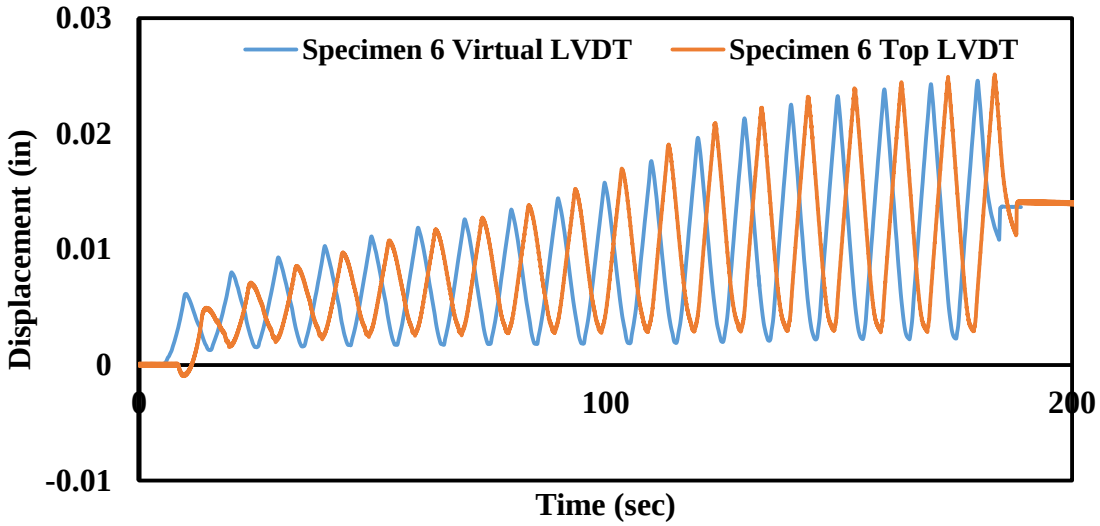

Figure A2 Cyclic Displacement of Specimen 6

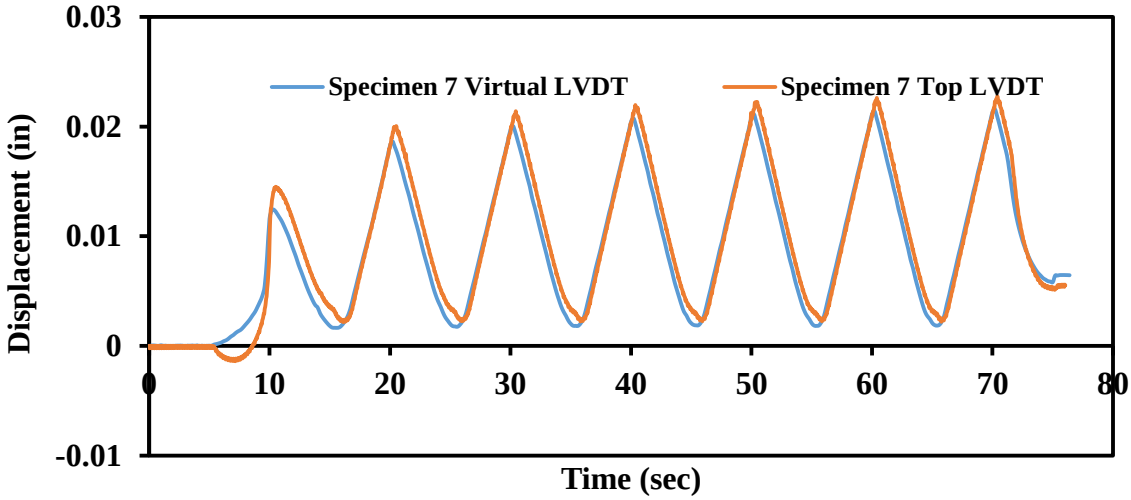

Figure A3 Cyclic Displacement of Specimen 7

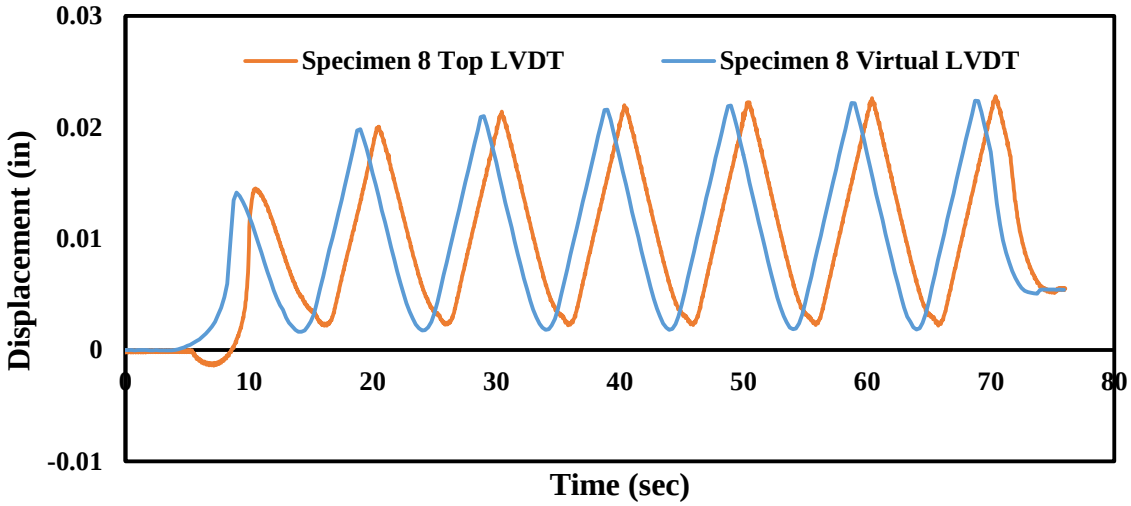

Figure A4 Cyclic Displacement of Specimen 8

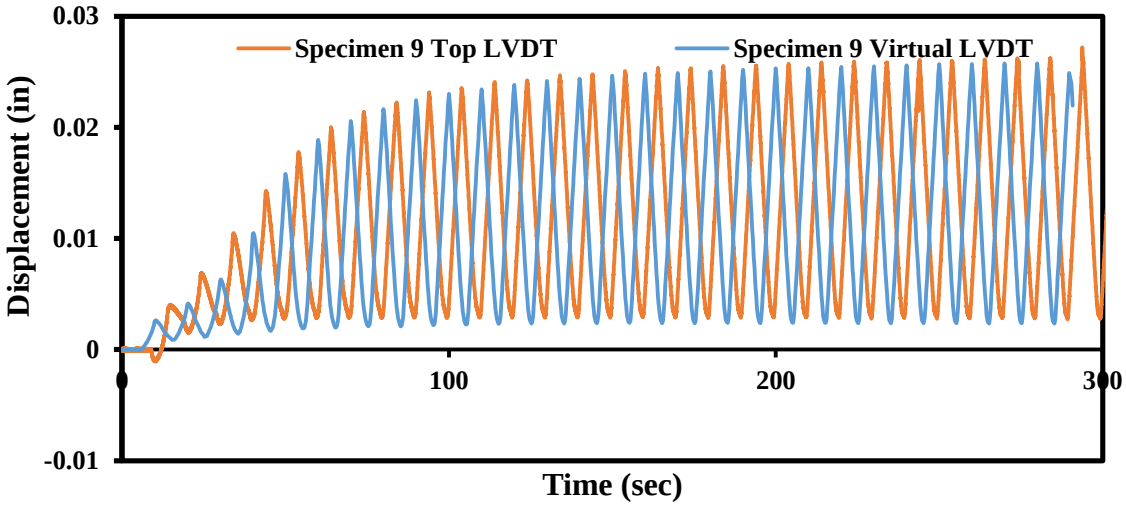

Figure A5 Cyclic Displacement of Specimen 9

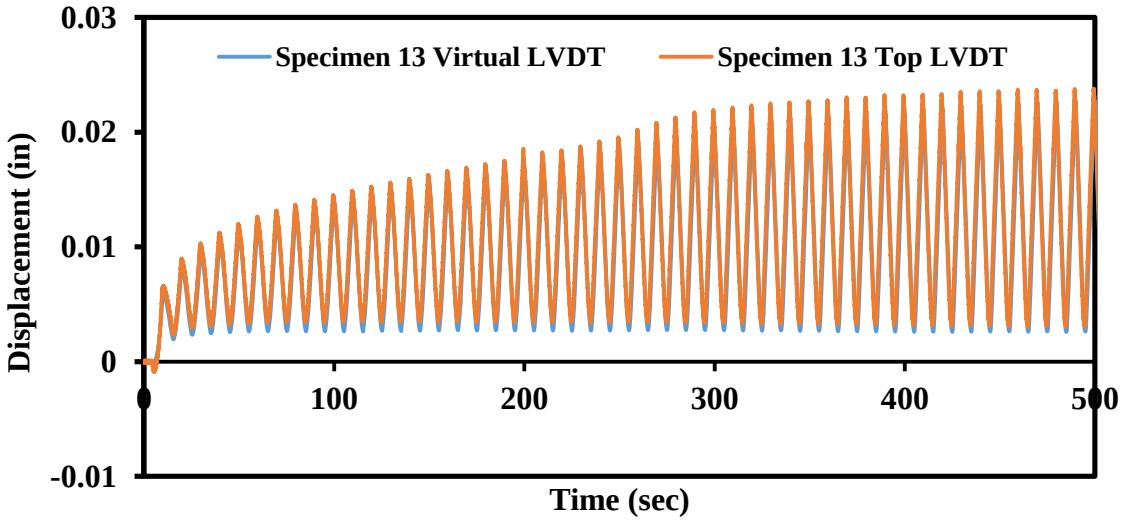

Figure A6 Cyclic Displacement of Specimen 10

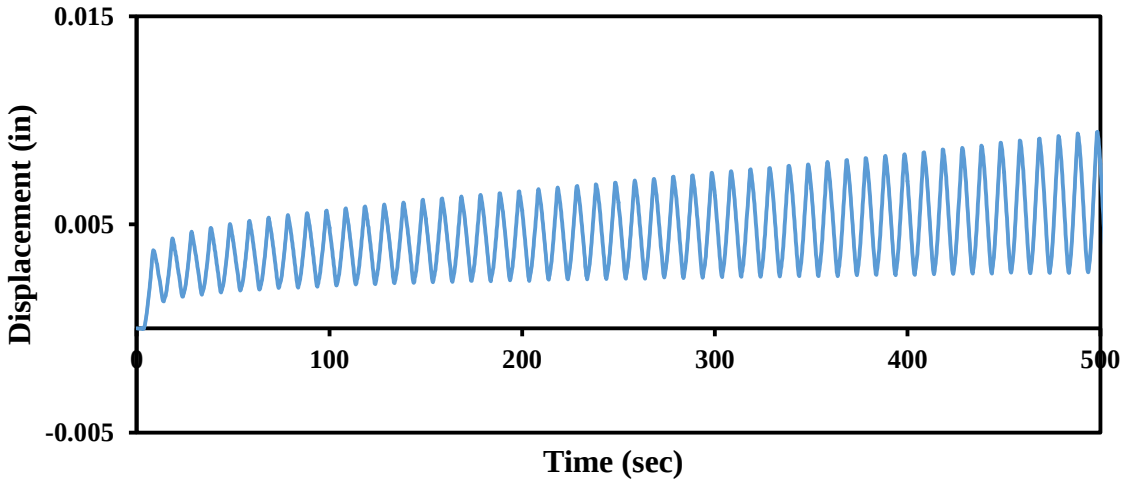

*Data not available for top LVDT

Figure A7 Cyclic Displacement of Specimen 14

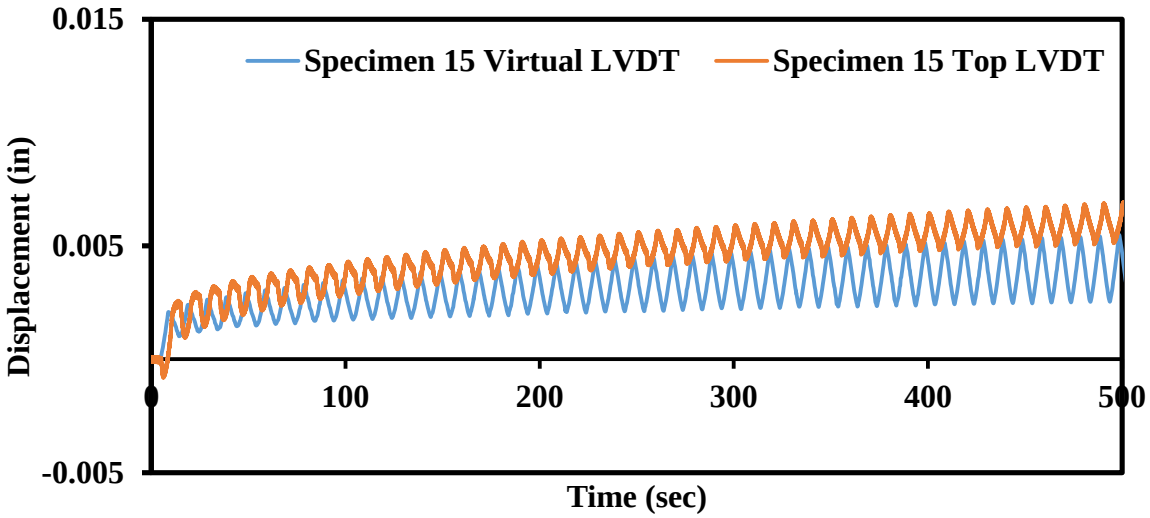

Figure A8 Cyclic Displacement of Specimen 15

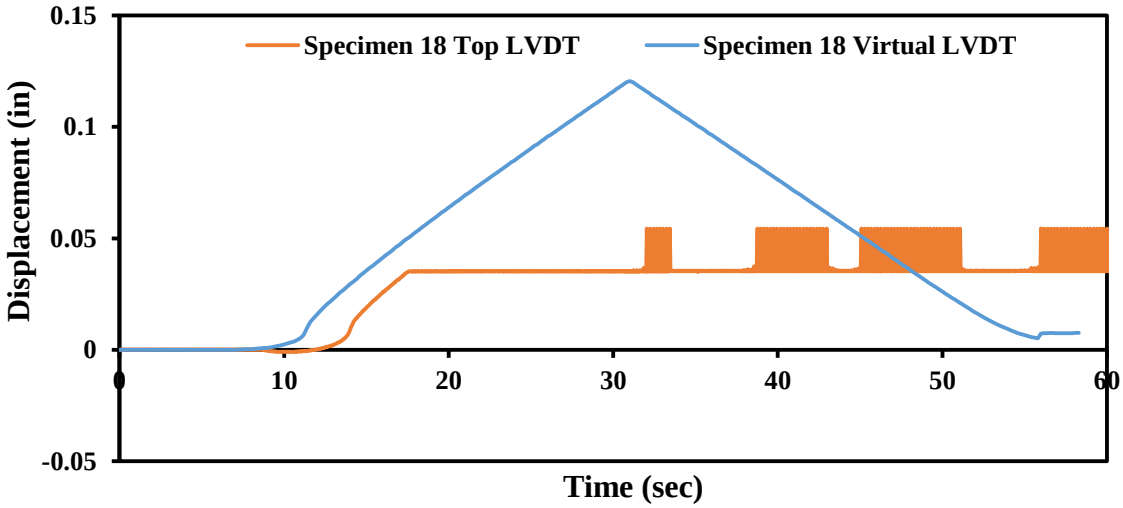

Figure A9 Monotonic Displacement of Specimen 18

Vita

Estefany Ramos was born in El Paso, Texas, and graduated from Loretto Academy High School in 2009. She attended the University of Texas at El Paso to pursue a Bachelors in Civil Engineering and received her degree in the fall of 2013. She became very involved in the student chapter of the American Society of Civil Engineers (ASCE) and became president of the organization in 2013. She entered the master's program at UTEP in the spring of 2014. While pursuing her master's degree, she began working as a research assistant at the Center for Transportation Infrastructure Systems (CTIS) and had the opportunity to perform research in the area of asphalt testing.

Permanent address: 12071 Bach Way
El Paso, Texas, 79936

This thesis was typed by Estefany Ramos